CRITICAL ISSUES FOR THE DEPLOYMENT OF PLASTIC WASTE PYROLYSIS

Emanuele Giglio[1], Alessia Marino[1], Patricia Pizarro[2,3], José M. Escola[3], Massimo Migliori[1], Girolamo Giordano[1], David P. Serrano[2,3*]

[1]*Chemical Engineering and Catalysis for Sustainable Processes (CECaSP) Laboratory, University of Calabria, Via Pietro Bucci, 87036, Rende, Italy.*

[2]*Thermochemical Processes Unit, IMDEA Energy Institute, Avenida Ramón de la Sagra, nº 3, 28935, Móstoles, Madrid, Spain.*

[3]*Group of Chemical and Environmental Engineering, Rey Juan Carlos University, c/Tulipán s/n, 28933 Móstoles, Madrid, Spain.*

**Corresponding author:*

E-mail address: david.serrano@imdea.org

Abstract

Despite the urgent need to valorize plastic waste, subtracting them from uncontrolled release into the environment, and the availability of consolidated thermal and catalytic technologies, the large-scale deployment of pyrolysis as a reference technology for the efficient processing of plastic waste still faces significant challenges. Accordingly, this review is focused on a number of issues that are essential for the industrial development of plastic waste pyrolysis technologies: i) the use of heterogenous catalysts for a better control of the product properties and the softening of the operation conditions, analyzing the important limitations derived from catalyst deactivation, ii) the different types of treatments investigated for the safe removal of halogens, which are often present in the pyrolysis oils in the form of Cl- and Br-containing organic compounds, thus avoiding health and environmental problems and the corrosion of equipment, iii) the co-processing of plastic waste with other feedstocks (biomass, petroleum fractions, used tires, etc.), which may result in significant synergistic effects, and iv) the multi-scale modelling of plastics pyrolysis processes as an essential tool for the design of large scale plants.

Keywords: plastic waste, pyrolysis, dehalogenation, feedstock recycling.

1. Introduction

While plastics have become essential materials in our life, their manufacture requires high energy and raw materials consumptions. Moreover, their disposal at the of the lifecycle has become an issue of increased concern due to the strong environmental impact of plastic wastes. Thus, once the waste plastics reach the environment remain for decades due to their high stability and resistance against degradation. The environmental impacts are strongly enhanced in the case of microplastics (both primary and secondary) that may present particle sizes quite below 5 mm.

According to the first Global Plastic Outlook by the OECD [1], the generation of plastic was doubled between 2000 and 2019 reaching a value of 353 million tons. Focusing on the distribution of plastic waste generation in Europe, packaging industry accounted for about 60 % of total production, whereas electric/electronic, buildings/construction, agriculture and automotive sectors shared approximately the same percentage of total plastic waste generation (≈ 5 % each) [2].

The major technical challenges towards the 'Zero Waste goal' for plastics are related to the separation/sorting techniques and to the waste composition. A plastic waste stream usually consists of many different polymers with low compatibility, hence their separation into individual fractions is often required for their recycling. Moreover, contamination by other materials, as it occurs in the municipal solid wastes. represents an issue than hinders the achievement of zero waste targets for plastics [3]. In this way, a great part of waste plastics is contained within the municipal waste stream, which is a strong limitation for their recovery and recycling. Typically, a hierarchical approach is considered for the management of plastic wastes according to the following priority order: reduction of the generation, reuse of the spent goods, recycling, energy recovery and controlled disposal.

Currently, the most common way to recycle plastics is the so-called mechanical recycling that allows their re-processing into other plastic goods. It consists of a number of steps like collection, sorting, washing, grinding and extrusion. The main challenges of mechanical recycling deal with polymers degradation, mixing and contamination, hence in many cases the recycled plastic materials present low quality, which limits strongly their application [4]. Moreover, mechanical recycling cannot be

applied to thermostable plastics. Alternatively, feedstock recycling of plastic waste has emerged as a very interesting route that involves its transformation into non-plastic products.

Among the different thermochemical processes available for the conversion of plastic waste, pyrolysis is one of the most promising routes. Plastics pyrolysis involves their decomposition in an inert atmosphere operating at intermediate temperatures (typically in the range 400 – 600 ºC). Pyrolysis enables a high yield of the organic liquid fraction that can be exploited to produce fuels and/or raw chemicals, being recognized as a relatively simple and highly versatile technology. In this way, pyrolysis can be applied to plastic wastes with complex compositions or even to mixtures of plastics with other materials. When the pyrolysis products are intended to be used as fuels this approach should really be considered as indirect energy recovery, having some advantageous in terms of both efficiency and environmental impact in comparison with the direct incineration of the plastic wastes. Nevertheless, the most interesting route at present is the use of the pyrolysis fractions for the production of raw chemicals, which can be really classified as (chemical or feedstock) recycling. Pyrolysis of plastic waste has been deeply covered by the scientific community during last decades also with some important reviews, upgrading progressively the progress of the research in this field. The attention was focused on some specific technical aspects: from the early works focused on thermal pyrolysis [5] quickly the attention moved to the use of catalytic [6–9] exploiting the assessment of different catalyst[10] and the role of process conditions in deactivation. Also the product composition was considered in the view of process implementation at industrial scale[11,12] as well as effect of the waste characteristics to the process efficiency[13] was a topic well exploited in the literature as well as the techno-economic assessment of the process. However, despite the fact that also recent reviews summarizes new trends in process development [14–16], also from a up-to-front engineering perspective[17], there are still some of critical issues that should be rationalized in the view of commercial deployment of thermal and catalytic processes of plastic waste pyrolysis. With the particular perspective of future full development, the process at industrial level, beside the evaluation of recent evidence of thermal and catalytic pyrolysis and co-pyrolysis, some of those open questions

have been addressed in this review. This is the case of the strategies to reduce the impact of the presence of hetero-atoms (mainly halogens) in the waste-plastic and of a comprehensive multiscale modeling approach, as illustrated in Figure 1.

Advantages of catalytic pyrolysis versus thermal decomposition processes in terms of softer conditions and narrower product distribution is covered in section 2, addressing the important issue of catalyst deactivation that may strongly limit the feasibility of using catalysts for promoting the pyrolysis of plastic waste. Likewise, since the presence of halogenated compounds in plastic goods is a relevant problem, section 3 reviews a variety of strategies that have been investigated to reduce the halogen content in the pyrolysis oil. Another important aspect is the quality of the feed since very often it is contaminated containing materials other than plastics that could in principle interact either with synergistic or negative effects during the pyrolysis process. Accordingly, co-pyrolysis of waste plastics with other types of materials is covered in section 4. As final topic, section 5 discloses works published on multiscale modelling, including economic aspects, of plastic waste pyrolysis process. This is an essential area for supporting the scale-up procedures and the reliable estimation of pyrolysis process profitability at industrial scale.

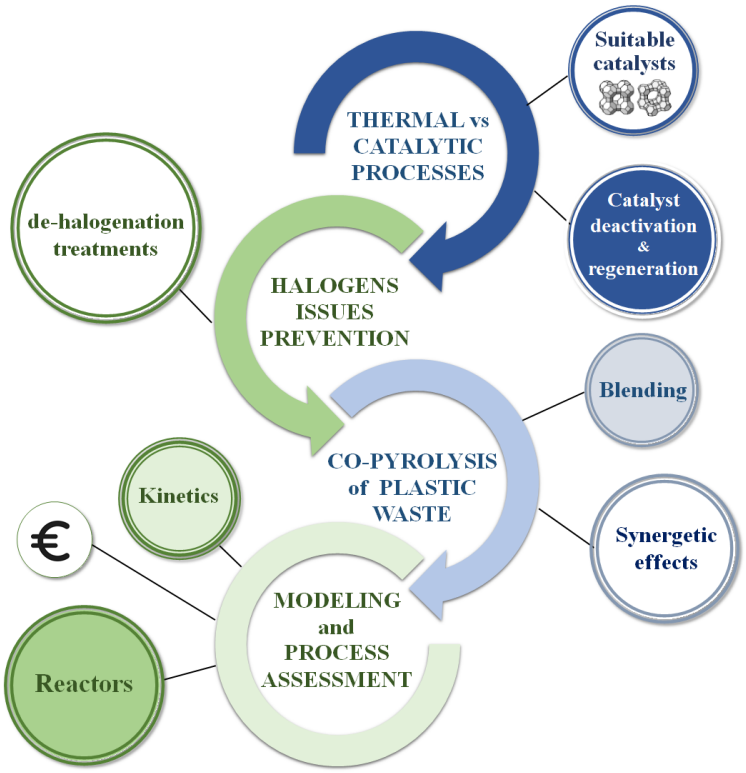

Figure 1. Main aspects for affording industrial plastic pyrolysis processes.

2. Thermal and catalytic pyrolysis of plastic waste

Thermal pyrolysis of plastics usually results in a broad distribution of products, which has limited commercial value. In contrast, the addition of a catalyst leads to a narrower and upgraded product distribution, as well as it improves the conversion, allowing the pyrolysis to be carried out at lower temperature. Thus, by designing conveniently the properties of the catalyst it is possible to drive the plastic conversion process towards different products with commercial applications (gaseous olefins, gasoline, diesel, waxes, or carbon materials). Figure 2 illustrates this concept, highlighting the most convenient route depending on the type of product to be obtained.

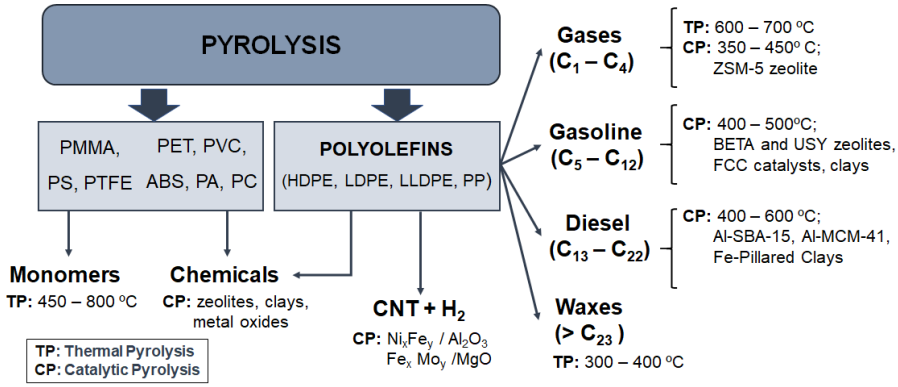

Figure 2. Main products that can be derived from thermal/catalytic pyrolysis of plastic waste.

2.1. Thermal pyrolysis

Thermal pyrolysis of plastics is governed by a few parameters, such as temperature, heating rate and residence time. Normally, temperatures in the range of 400-700 ºC are used under inert atmosphere and pressures close to the atmospheric one [5]. For polyolefins, at low pyrolysis temperatures (about 400 ºC), the main product is a heavy wax. In contrast, when temperature increases above 400 ºC, lighter products such as gaseous hydrocarbons and oils are also obtained [11,12]. At high pyrolysis temperatures, the share of gaseous hydrocarbons tends to hike at the expense of the oil production. On the other hand, the product distribution is strongly influenced by the reactor type. In this regard, during the thermal cracking of LDPE in a screw reactor, lower output of gases and higher yields of wax and oil were attained in comparison with a semi-batch system[18]. The screw reactor provided a

quite uniform residence time distribution, which avoided the extension of overcracking reactions in contrast with it occurred in the semi-batch system.

It is generally accepted that polyvinyl polymers, such as polyethylene (PE), polypropylene (PP) and polystyrene (PS), thermally decompose through a chain radical mechanism[19,20]. The random cleavage of the chain backbone leads to the production of both radical and stable species, progressively reducing their molecular weight. These polymers decompose according to bond cleavages occurring mainly within the backbone, with little involvement of side functional groups (hydrogen, methyl or phenyl group for PE, PP and PS, respectively). Random scission is the main initiation step that proceeds by C-C bond cleavage along the polymer backbone leading to the formation of two end-chain radicals. Propagation reactions can be generally grouped into two types: β-scission and H-abstraction of intermediate radicals. β-scission is a cleavage of the β-position bond, whilst H-abstraction can be intermolecular (i.e., it occurs between a molecule and a radical species) or intramolecular. Termination reactions involve the reaction between two end chain radicals forming a stable molecule.

In the case of polyethylene, this radical mechanism results in a broad hydrocarbon distribution in terms of carbon atom number. Interestingly, each fraction is made up mostly by the respective alkane, 1-alkene, and diene, since the occurrence of branching transformations is precluded [21]. In this regard, the highest yields by groups obtained in the thermal pyrolysis at 400 ºC in a batch reactor of the main polyolefins (LDPE, HDPE and PP) were for gasolines (C_5 – C_{12} hydrocarbons) with the following shares: 45%, 39% and 58%, respectively, followed by light diesel (C_{13} – C_{18} hydrocarbons) with yields of 32%, 33% and 18% as well. It is also noteworthy the huge amounts of olefins present in the liquids according to their bromine index measurements: 54.1 (LDPE), 64.6 (HDPE) and 83.8 (PP) g Br_2 / 100 g sample[22]. Nevertheless, for a few polymers, thermal pyrolysis leads to a high selectivity towards the constituent monomer. These are the cases of polymethyl methacrylate (PMMA), polystyrene (PS) and polytetrafluoroethylene (PTFE)[23]. Thus, for PS, its thermal cracking in a flow reactor at 350 ºC led towards 80.1% oils containing 70% of styrene monomer[24]. On the other hand,

for the case of PET, which is another commodity plastic, its thermal cracking at 550 ºC in a fluidized bed resulted in a great deal of gases (49.1%), being formed mostly by carbon oxides ($CO + CO_2 >$ 90%), while the share of liquids and solids were 39.4 and 12.8 %, respectively. Interestingly, the major components of the liquids were benzene and toluene[25]. Likewise, the thermal cracking of polyamides (PA) and polyurethanes (PU) in a fluidized bed at 760 ºC gave rise to significant amounts of gases (39.2 and 37.9, respectively) although the main product in both cases were a mixture of oil and wax (56.8 and 56.3 %). In contrast, with polycarbonates (PC) at 710 ºC, less gases were produced (26.5 %) with liquids again as main products but obtaining significant amounts of char (24.6 %) as well[23]. It should be borne in mind that , these polymers are thermally decomposed into different nitrogen and oxygen-containing species and some of them finally end up in the oil fraction. Several of these compounds can be interesting as raw chemicals, thus affording the circularity of plastic waste.

2.2. Catalytic pyrolysis

The different catalytic pyrolysis treatments may be classified into two groups (in-situ and ex-situ) that refer to whether it exists or not, respectively, a direct contact between the plastics and the catalyst in the reaction medium.

The in-situ treatments are more prone to undergo catalyst deactivation caused not only by carbonaceous deposits (e.g., coke) but also by the presence of diverse impurities contained in the plastics refuse. Additionally, the subsequent separation of the catalysts from the remaining solid residue (char) after reaction is more difficult as well, hindering the catalyst recovery and reuse. Owing to these facts, the in-situ treatments have been mostly investigated with virgin plastics with the aim of investigating the performance of the different catalysts in plastic pyrolysis.

In contrast, ex-situ treatments are featured by the existence of two separate stages consisting of a first thermal degradation of the raw plastic mixture followed by the catalytic upgrading of the products coming from the first step. The ex-situ system can be coupled to process directly the vapors produced in the thermal treatment or, alternatively, such vapors can be condensed in the form of oil or waxes that can be storage, purified and transported long distances to be subjected finally to the catalytic

upgrading step. In the ex-situ setup, the catalyst undergoes less deactivation by solid carbon deposition and besides, it exists the possibility of removing non-desired components before coming into contact with the catalyst, that attenuates its deactivation and facilitates the integration of the process into a refinery [26]. On the other hand, in the ex-situ setup, the catalyst can be easily retrieved from the reactor and regenerated which enables its reuse. These facts render the ex-situ treatments especially suitable to deal with real plastic wastes, being the preferred option for the large-scale industrial application of catalytic pyrolysis with true plastic wastes.

The great advantage of catalytic pyrolysis is that by a convenient selection of the catalyst type and its properties, the plastic pyrolysis process can be selectively directed to different types of products with industrial interest: liquid mixtures of hydrocarbons to be used as fuels, light olefins that could be employed as raw chemicals, hydrogen, and even high value carbon nanomaterials. Additionally, the techno-economic viability of catalytic pyrolysis of plastic wastes has been proved, provided that the plastics refuse prices remain low, especially for the plants having a high operational capacity [16].

Plastics cracking on acid catalysts follows a carbocationic mechanism. It usually proceeds in the initial reaction steps via carbenium ions produced by the abstraction of a hydride ion (Lewis acid sites) from the polymer or by the addition of a proton (Brønsted acid sites) to the polymer forming a carbonium ion. Subsequently, carbenium and carbonium ions decompose resulting in the formation of shorter alkenes or alkanes, respectively, and additional cations of lower molecular weight which undergo further cracking. Unstable cations can generate stable molecules via recombination, disproportionation, cyclization, isomerization, hydrogen transfer, aromatization or polycondensation (i.e., cyclic alkanes/alkenes and aromatics are formed) [27]. In addition, linear compounds (typical of thermal degradation) are also produced simultaneously.

The main catalysts used in both in-situ and ex-situ catalytic pyrolysis are zeolites, mesoporous aluminosilicates, clays and metal compounds supported over different carriers.

Zeolites are crystalline microporous aluminosilicates with a pore size below 1 nm showing an acid site distribution of both Brønsted and Lewis acid sites, whose amount and strength depends on the

aluminum content and the zeolitic structure. Thus, different zeolites have been tested in the catalytic cracking of polyolefins such as ZSM-5, Beta, USY, Mordenite and others structures[28–41]. The incorporation of the zeolitic catalysts ramps up the conversion with respect to thermal cracking and also changes the selectivity pattern in polyolefin cracking. The product distribution is shifted towards a narrower one formed by lighter products with a different composition, favoring the formation of aromatics and branched hydrocarbons by carbocationic reactions[42–44]. As a general trend, the share of gaseous hydrocarbons increases with the acid strength of the zeolite. Thereby, over ZSM-5 zeolites, which contains strong acid sites and a small micropore size (about 0.55 nm), yields of C_2–C_4 hydrocarbons above 60 % have been reported, made up mostly by olefins, while the liquids contain significant amounts of monocyclic aromatic hydrocarbons[28,29,37,39,41,45,46]. Additionally, ZSM-5 suffered lower deactivation than other zeolites with larger micropore (Beta, HY) due to the hindered growth of the coke precursors into its micropore structure. In contrast, over zeolite USY, liquid hydrocarbons within the gasoline range were found as the main products due to both its larger micropore size (≈ 0.73 nm) and weaker acidity than ZSM-5 [31,35,36]. Likewise, FCC catalysts, which are based largely on zeolite Y, gave rise to high gasoline yields as well (above 80%) [47]. Both Lewis and Brønsted acid sites of the zeolite are involved in the cracking process, although the latter seems to play a leading role. Hence, the high C_2-C_4 selectivity shown by ZSM-5 was ascribed to the large extent of end-chain cracking reactions taking place mostly over the strong Brønsted acid sites of the zeolite[48].

A particularly important issue to tackle with in the catalytic conversion of plastics is the bulky feature of the polymers, which results in the appearance of severe diffusional and steric hindrances in small pore catalysts, such as zeolites. Therefore, catalysts with high accessibility in terms of both pore size and surface area are highly recommended for the processing of the polymers [49]. In this way, the use of conventional micrometer size zeolites with small micropores (e.g., ZSM-5) in the cracking of bulky polyolefins resulted in lower activities due to transport limitations. To solve this problem, nanosized zeolites with a crystal size within 10-80 nm were successfully harnessed, due to their increased share

of external acid sites, fully accessible to the polyolefins, providing higher cracking activities [50–54]. A step forward in this direction of enhancing the active sites accessibility to facilitate polyolefin cracking was the application of hierarchical/mesoporous zeolites. They are characterized by possessing a bimodal microporous/mesoporous pore size distribution, whose nature depends on the synthesis method [51,52]. The enhanced accessibility of the hierarchical zeolite resulted typically in higher polyolefin cracking activities [55–59].

Additionally, the introduction of a CO_2 atmosphere instead of N_2 in the LDPE catalytic pyrolysis over metal (Fe, Ni, Co, Mn, Ag, Cu) -modified mesoporous HZSM-5 increased meaningfully the selectivity towards aromatics [60].

In addition to zeolites, other materials showing weaker acidities have been also tested in plastics catalytic pyrolysis to increase the share of liquids. Thus, a number of clays have been explored[61,62]. Saponite and montmorillonite have shown higher yields of liquids (70 %) than USY zeolite (50 %), being most of them in the range of gasolines while an Fe-pillared clay led to a great deal of diesel range hydrocarbons (80.5 %). Likewise, the catalytic pyrolysis of waste LDPE packaging over 2 wt.-% magnesium bentonite at 340 ºC resulted in about 70 wt.-% of liquids with similar properties to petroleum diesel in terms of its high cetane number, heating value and low viscosity. Interestingly, the latter clay catalyst, considering its makeup, is meant to contain both acid and basic sites [63].

Al-MCM-41 and Al-SBA-15, characterized by the presence of uniform mesopores and a mild acid strength due to the amorphous nature of their pore walls, have been also tested in polyolefin cracking. Thus, the enhanced accessibility of Al-MCM-41 increased the kinetics for the catalytic cracking of LDPE/HDPE and, especially, PP [49,64–66]. Additionally, in PP cracking at 400 ºC over Al-MCM-41, high selectivities towards gasolines (C_5 – C_{12}) were achieved (65%), obtaining also meaningful selectivities to light diesel hydrocarbons (C_{13} – C_{22}), around 20%. For LDPE and HDPE cracking over Al-MCM-41, the main products were gasolines as well although in slightly lower amounts (52 – 63%), chiefly made up of olefins and isoparaffins and with little content of aromatic hydrocarbons[65].

Although ex-situ systems represent a more feasible option for the catalytic pyrolysis of waste plastic, they have been less investigated in the literature. In this way, it is noteworthy that ex-situ catalytic pyrolysis of polyolefins over HZSM-5 zeolite has unveiled meaningful differences in the attained product distribution with regards to the in-situ process harnessing the same catalyst [41,67–70]. Thus, over nanosized HZSM-5 at 450 º C, higher yields of gaseous products (74 wt.-%) were obtained in the catalytic reforming of LDPE that were made up primarily of C_2 - C_4 light olefins [41]. In another study [67], the in-situ catalytic pyrolysis of LDPE and PP at 600 ºC led towards more aromatics and solid carbon residues than the ex-situ process. Interestingly, the ex-situ catalytic pyrolysis gave rise to a huge augment in the C_2 – C_4 olefins yields reaching up to roughly 80 %, instead of the approximate 30% for the in-situ treatment.[63] In general terms, these results hold promise considering the industrial application of ex-situ catalytic pyrolysis of polyolefins. Table 1 summarizes the main commented features of the catalysts used for polyolefin cracking:

Table 1. Main features of the catalysts used in the catalytic pyrolysis of polyolefins

Catalyst	Advantages/disadvantages	Plastic	Main product	References
Conventional HZSM-5 zeolite	High acid strength Reduced accessibility by its low micropore size Lower cracking activity with bulky polymers (PP)	HDPE, LDPE	~ 60 – 70 % C_2 – C_4, mostly olefins, 5 – 15% MAH in liquids Lower coke yields	28,29,46,65,68
Nanosized HZSM-5	High acid strength Good accessibility by its high external surface area High cracking activity	LDPE	70 – 80 % C_2 – C_4, mostly olefins	41
Hierarchical HZSM-5	High acid strength	LDPE, PP	60 – 80 % C_2 – C_4, chiefly olefins 4 – 15% in liquids	48,54,59,68,70

	Improved accessibility by its bimodal (micro/meso) pore size distribution Higher cracking activity			
HUSY zeolite	Medium acid strength Large micropores and cages	HDPE, PP	50 – 80 % gasolines, higher amount of saturated hydrocarbons Higher coke yields	33,35,37
FCC catalyst	Mixture zeolite USY plus other components (mostly silica-alumina) Medium acid strength Better accessibility	LDPE	70 - 80% gasolines High aromatic content (20 – 50%)	47
Zeolite HBeta	High/medium acid strength Large micropore	LDPE, HDPE, PP	60 – 70% gasolines	45
Al-MCM-41, Al-SBA-15	Medium acid strength High accessibility by its uniform mesoporosity	LDPE, HDPE, PP	50 – 65% gasolines	49,65
Clays/Pillared Clays	Weak acid strength Large micropores	LDPE	50 – 70% gasolines, High olefin content	61,62

Other polymers different from polyolefins have also been converted by catalytic pyrolysis. Hence, both PA and PUR were decomposed over HUSY and NH_4NaY zeolites at 500 ºC in a pyrolizer coupled to GC-MS [71], leading to mixtures with a significant concentration of potentially valuable N-containing compounds, such as hexanedinitrile, aniline, p-toluidine, pyrrols and pyrrolidines, in

addition to a variety of aromatic hydrocarbons. However, PUR catalytic pyrolysis has been focused primarily on the removal of N-containing pollutants such as NH_3 and HCN converting them into gaseous N_2. To this end, CaO has proved to be particularly effective increasing three-fold N_2 yields and making disappear virtually HCN[72]. On the other hand, the presence of EVA copolymers resulted in the quick deactivation of both Al-MCM-41 and Al-SBA-15 by the generation of unhindered crosslinked structures, finally leading to coke [73]. Polycarbonates were also subjected to catalytic pyrolysis over both Zr and Fe supported oxides over zeolite HY at 650º C [74]. The addition of Zr increased the share of aromatic hydrocarbons (particularly monocyclic ones) by its higher content of Lewis acid sites (oxygen vacancies), which facilitated the deoxygenation of phenolic products. Hence, over Zr/HY, the share of monocyclic aromatics (e.g. benzene, toluene, xylenes, ehylbenzenes, etc.) augmented from 19.3% (non-catalytic) to 36.4% while those of phenolics dropped from 70.1% (non-catalytic) to 52.2%[75]. In the case of PET, its catalytic pyrolysis over ZSM-5 at 600 ºC promotes decarboxylation reactions leading mostly towards benzene (5%), benzene derivatives (3%) and indenes/naphthalenes (3%). This product makeup differs heavily from that obtained in the thermal pyrolysis which resulted chiefly in benzoic and acetylbenzoic acids (20%) with low amounts of benzene and benzene derivatives (< 1.5%). Interestingly, CaO, that is a basic oxide, also enhanced decarboxylation and produced even more benzene (7%) than ZSM-5 in the catalytic pyrolysis of PET at 600 ºC, at the expense of generating less yields of benzene derivatives and indenes/naphthalenes[76,77].

In addition to hydrocarbon mixtures, other interesting products (hydrogen and carbon) can be obtained by catalytic pyrolysis of polyolefins. In this regard, different metals supported on carriers of diverse nature have been investigated. Thus, bimetallic Ni_x-Fe_y supported over γ-Al_2O_3 allowed to obtain high yields of both carbon nanotubes and hydrogen from real plastic waste in an ex-situ configuration reactor [78]. The remarkable performance of this catalyst was ascribed to its improved interaction with the support which favors the dispersion of bimetallic Ni_x-Fe_y particles. A similar process comprising firstly pyrolysis of LDPE over ZSM-5 followed by the catalytic decomposition

of the obtained hydrocarbons over Fe_xMo_y supported on MgO also resulted in high yields of carbon nanomaterials. Interestingly, the type and morphology of the latter depended distinctly on the Fe/Mo ratio over the MgO support [79].

2.3. Catalyst deactivation and regeneration

During catalytic pyrolysis of plastic waste, the catalyst may suffer strong deactivation, which is one of the major limitations for this type of process to be applied at large scale. As illustrated in Figure 3, the main pathways identified for the catalyst deactivation during plastic cracking correspond with coke deposition, formation of Al extra-framework species and acid sites poisoning.

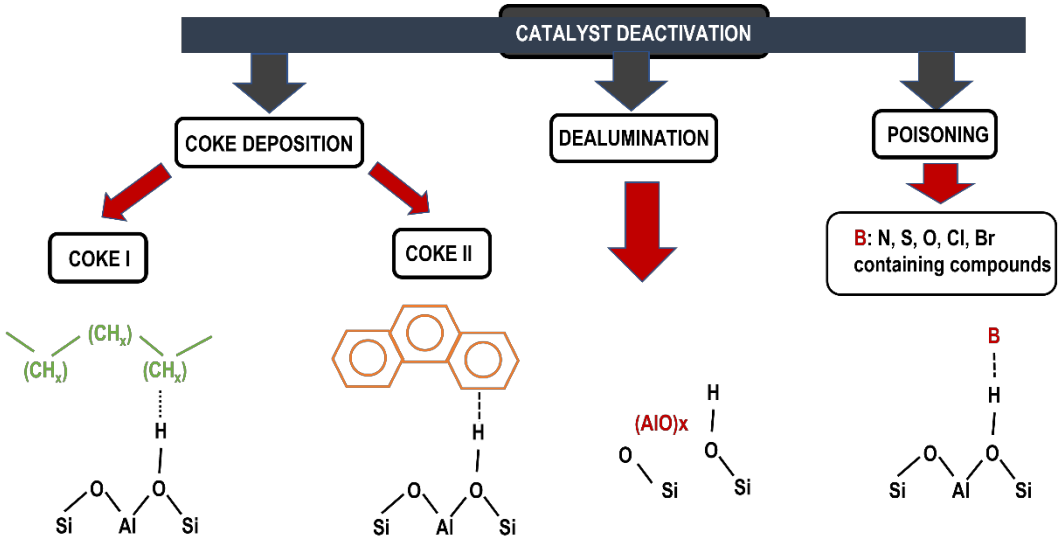

Figure 3. Deactivation types of acid catalysts used for plastics pyrolysis.

Coke is formed by means of several cooperative reactions (cyclization, hydrogen transfer, oligomerization, dehydrogenation, and aromatization) which are catalyzed by the zeolite acid sites [30,80,81]. The deposition of coke not only abates the activity of the zeolitic catalyst but also results in a substantial modification of the product distribution. For instance, a reduction of the yields of aromatics and paraffins, due to the acid sites deactivation, which restricts hydrogen transfer reactions, has been reported [82,83]. It is noteworthy that the physicochemical properties of the catalyst are heavily affected by coke deposition [80]. In terms of acidity, the strong acid sites are more quickly deactivated by coke while weak acid sites remain virtually unaffected [82]. In addition, both Brønsted and Lewis acid sites are blocked by coke deposition although the former are affected in a larger extent [80].

Two kinds of coke were observed over deactivated MFI zeolite after HDPE catalytic pyrolysis: coke I, whose maximum combustion rate in TGA experiments was placed at 440-460 ºC and coke II, wherein the maximum rate occurred at higher temperature (520-540 ºC) [82]. Coke I is considered to contain higher amounts of aliphatic groups while coke II shows a larger share of aromatic groups. Additionally, coke I is expected to be placed preferentially over the external surface of the zeolite. In contrast, coke II is meant to be present mostly inside the zeolite micropores.

The amount of deposited coke is largely bound up with the micropore size and the share of mesopore/external surface. Thus, the larger the micropore size (D_p) of the zeolite, the higher the amount of deposited coke, as the growth of coke precursors is less constrained, as it is the case of ZSM-5 zeolite [30,31]. It is also noteworthy that hierarchical ZSM-5 showed enhanced tolerance to deactivation with regard to conventional ZSM-5, highlighting the importance of mesoporosity to slow down the zeolite deactivation by the fast removal of coke precursors [68].

Coke deposition is usually a reversible event since the catalyst can be regenerated by oxidation with air or oxygen [84]. However, there is a temperature limit for the regeneration treatment to avoid loss of both crystallinity and textural properties of the catalyst. Additionally, care should be taken if steam is present at temperatures above 450ºC. This causes dealumination of the zeolite framework, transforming Brønsted acid sites into Lewis sites, which may negatively affect the catalytic activity.

On the other hand, during the catalytic pyrolysis of plastic waste, poisoning of the acid sites may occur, mostly related to the presence of N and/or S but also by O and halogen containing compounds in the feedstock. This fact was observed in the catalytic cracking of a 70/30 (%w/w) LDPE-lubricating oil base mixture, the latter containing meaningful amounts of both N and S. This fact led to an activity decay at 400/450 ºC for Al-MCM-41, so higher temperatures (450/500ºC) were required to attain full conversion [85].

3. Pyrolysis of halogen-containing plastic waste: dehalogenation treatments

Halogen-containing compounds are widely used as additives to improve mechanical, electrical, chemical, and thermal properties of plastic goods. In addition, halogens can be incorporated into plastics through reactive monomers. This is the case of polyvinyl chloride polymer, which is the main chlorine source in waste plastics as it contains about 58 wt.% of Cl. Bromine is instead mostly present in the form of Brominated Flame Retardants (BFRs). An additional contribution to the presence of halogens in plastic waste is related to salts arising from both contamination and the plastics separation process by flotation/sedimentation in saline solutions.

Accordingly, the presence of halogens represents one of the main issues to be faced in plastics thermo-chemical conversion, which affects both process management and pyrolysis products to be used in the recovery chain. With particular regard to pyrolysis oil, a maximum halogen concentration of 50 ppm is required to be used as fuel according to Stockholm Convention (2015) [86]. That is because, as a result of combustion, the organohalides present in the pyrolysis oil can be partially oxidized to form toxic and carcinogenic polyhalogenated dioxins. Additionally, hydro-halogen acids (dangerous for human health and corrosive to the industrial plants) can be released in the pyrolysis treatment or during its subsequent processing in petrochemicals units.

To address these specifications, different dehalogenation processes have been developed to be coupled to pyrolysis technology (Figure 4): dechlorination by thermal pre-treating (stepwise pyrolysis), in situ dehalogenation sorbent/catalyst-mediated, and ex situ upgrading of pyrolysis oil [87]. In addition, hydrodehalogenation technologies have been studied, which however fall outside the scope of this work but that have been covered in other review articles [88,89].

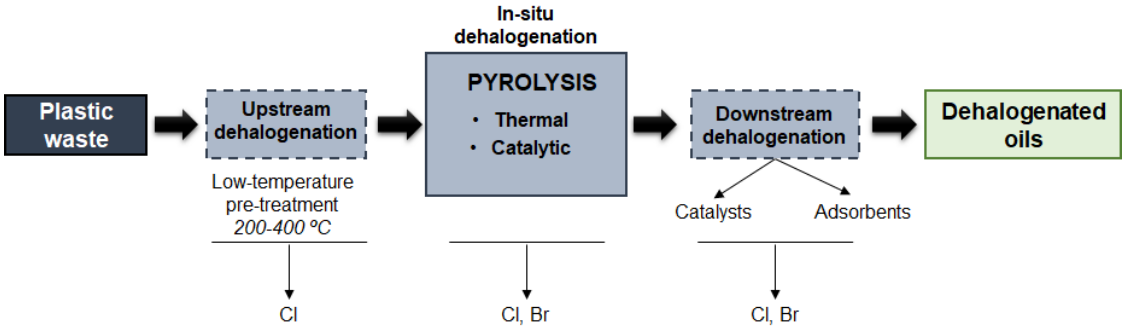

Figure 4. Plastic waste pyrolysis-associated dehalogenation processes.

3.1. In-situ dechlorination treatments

Among halogenated polymers, polyvinylchloride (PVC) is the most widespread. The high PVC chlorine content represents one of the main problems for the large-scale deployment of waste plastics pyrolysis processes. Based on the binding energies, the breaking order of the polymer bonds is C-Cl, C-H and C-C. Therefore, the early stages of thermal cracking are characterized by hydrochloric acid release from side-groups-elimination, resulting in an unsaturated chain [6]. On this basis, a preliminary low temperature dehydrochlorination step, generally carried out in the temperature range of 200-400 °C and in an inert atmosphere, is a good option to reduce the halogen content. This technological solution of a stepwise pyrolysis consists of a two-stage thermochemical process, wherein the dehalogenation treatment is followed by conventional pyrolysis [90]. The dehydrochlorination efficiency is related to the feedstock composition and reactor type, depending also on the reaction parameters, e.g., temperature and holding time.

Bockhorn et al. [91] investigated the stepwise pyrolysis of a pure polymers mixture (polyamide, polystyrene, polyethylene and polyvinylchloride) increasing the temperature up to 800 °C. Reported results indicated that hydrochloric acid release starts at 220 °C, with a maximum evolution rate at 280 °C, reaching the highest chlorine removal of 83 % at 400 °C. The influence of holding time and temperature was studied by López et al. [92]. The authors demonstrated that 99.2 % of the initial chlorine can be removed by treating a PVC-containing polymer mixture at 300 °C for 30 min, in a semi-batch reactor. Furthermore, distribution and composition of the subsequent pyrolysis products are affected

by the dehydrochlorination step, so that the stronger the treatment, the higher the gas yield and the heavier the hydrocarbons in the oil. This finding was also confirmed by Yuan et al. performing dehydrochlorination pre-treatment of pure PVC in a lab-scale gas-liquid fluidized bed reactor [93]. HCl release started during the melting stage and 300 °C was confirmed as the most efficient temperature, whilst a further increasing was accompanied by the polymer chain decomposition, resulting in an increment in light hydrocarbons production. In these conditions, up to 99.5 % of the initial chlorine was eliminated. An even higher dechlorination degree, equal to 99.86 %, was obtained by pre-treating pure PVC at 320 °C for 20 minutes in a fixed bed reactor, which then led to a low chlorine content oil, as well as rich in aromatics [94].

On the other side, a double-step process, consisting of a low temperature dechlorination pre-treatment followed by fast-pyrolysis, of a real waste PE/PVC mixture was investigated by Marino et al. [95].The authors demonstrated that the thermal treatment at 350 °C for 30 minutes can eliminate the 87 % of chlorine in form of HCl, safely stored.

Experiments at larger scale were carried out by Lei et al. [96], using a vented screw conveyor to continuously dechlorinate 1 kg/h of PVC-containing plastic waste with a stirred batch reactor, before the pyrolysis step. Investigating the effects of the residence time and the rotational speed at 300 °C, they concluded that long residence time and low screw speed favourably impact on the halogen removal efficiency (greater than 98%). Furthermore, all thermal and catalytic pyrolysis experiments resulted in low-chlorine oil and char since the evolved halogen was mainly accumulated in the gaseous fraction.

With the view to reaching a single-step process, dechlorination by thermal co-pyrolysis with adsorbents has been also investigated. The sorbent materials can trap the emitted HCl by adsorption, retaining it in the solid fraction. For the same purpose, a variety of catalysts and catalyst/sorbent composites have been tested, with the dual function of upgrading the pyrolysis products and inhibiting the hydrochloric acid release, including zeolites, calcium- and aluminium-based sorbents, Al-Zn composites, heavy metals, and metal oxides [97–102].

Calcium-based sorbents have been extensively studied for their ability to fix chlorine as $CaCl_2$. It has been demonstrated that in presence of CaO, a temperature of 500 °C represents the limiting operating parameter, since higher values lead to the volatilization of metallic chlorides [98]. The calcium chloride formation is also affected by both the chlorine species and vapour residence time inside the reactor and, therefore, by the inert gas flow rate. In fact, very short or long contact times of vapours with the sorbent bed can limit the $CaCl_2$ formation in favour of the generation of HCl and chlorinated hydrocarbons, respectively [99].

On the other hand, aluminium-based catalyst/sorbent composites have been also widely investigated. Aluminium, in form of Al_2O_3 or silica-alumina, has been found to have just a slight HCl fixing power, acting mainly as catalyst [102]. Instead, when composites sorbents were used, such as Red Mud [100] and Al-Zn Composite Catalyst (AZCC) [101], the chlorine concentration in pyrolysis oil dropped dramatically, denoting the ability of iron and zinc to fix chlorine in form of metallic chlorides.

The combined effect of stepwise pyrolysis and different sorbents was also studied by Hubáček et al., which pyrolyzed a model plastic mixture containing 10 % of PVC. The authors showed that thermal treatment at 350 °C, followed by the use of Fe_3O_4 as sorbent in an ex-situ configuration, allowed to drastically reduce the chlorine content in the liquid fraction [103].

3.2. In-situ debromination treatments

The main bromine source in waste plastic lays in Brominated Flame Retardants (BFRs), widely used as additives in plastic products to increase the fire resistance. Among the diversity of commercially available BFRs, Polybrominated Diphenyl Ethers (PBDE), Brominated Epoxy Resins (BE), Tetrabromobisphenol A (TBBPA), Hexabromocyclododecane (HBCD) and Polybromobiphenyls (PBB) represent the most used types. During pyrolysis, no early decomposition of BFRs is observed in contrast to what occurs in the same temperature range for PVC. Therefore, stepwise pyrolysis does not represent a suitable option for bromine removal [88] and the conventional way to address the debromination of pyrolysis products consists of incorporating sorbents to the pyrolysis process able to physically adsorb or chemically react with organobromines, bromine radicals and hydrobromic

acid, resulting from BFRs decomposition. In addition, it must be highlighted that BFRs are typically used in combination with antimony trioxide, which provides a synergistic effect as it is able to increase their activity by quenching the radicals formed during the combustion. Nevertheless, SbO_3 represents an additional pollutant present in these plastic wastes, which makes the achievement of contaminants-free pyrolysis products even more challenging.

Due to their double nature of catalyst and sorbent, zeolites have been widely investigated in catalytic pyrolysis in presence of brominated compounds under different operation conditions and feedstocks. Zeolite pores size plays a key role in the debromination efficiency. Thus, large pores in 13X and NaY led to the complete cracking of big BFRs that, in contrast, was inhibited by the partial pores inaccessibility of the molecular sieve 4A [104].

To enhance the debromination efficiency, iron-containing zeolites and composites were also tested in catalytic pyrolysis of BFRs-containing polymer mixtures [88,104–106]. It has been shown that iron oxide can react with HBr and bromine radicals to form brominated salts, inhibiting simultaneously the formation of volatile $SbBr_3$, and then avoiding its migration into the oil and enhancing the capture of both antimony and bromine in the pores of the sorbent. Nevertheless, the interaction between Fe and organobromines proved to be more effective than that with hydrobromic acid, so that both the reaction temperature and the catalytic effect of zeolites used as supports need to be tailored to avoid the complete cracking of BFRs in HBr. A further oil debromination was achieved (up to 95 %) by using mesoporous materials as iron supports, as the bigger channels allow access to larger organic bromides, improving the cracking by acidic terminal silanols [105]. In this way, also the interaction between iron oxide and antimony is enhanced, leading to a stronger Sb trapping in the sorbent, whereas the conversion of organobromines to coke is promoted due to the carbon solubility of metal oxides.

As for chlorine capture, Ca-based sorbents have been designed also in debromination processes. $CaCO_3$ and Ca-C composite were tested by Brebu et al., achieving a 40 % and 80 % reduction of Br in pyrolysis oil at 450 °C, respectively [106]. Likewise, Jung et al. demonstrated that the bromine

removal in oil increases in the order CaO, $CaCO_3$, $Ca(OH)_2$ (57.4, 65.5 and 75.4%), with a substantial enhancement of 83.4 % of antimony trapped in the solid residue when calcium hydroxide was used [107]. The mechanism of bromine trapping by calcium hydroxide was studied by Gao et al., integrating experimental pyrolysis of BE-containing PCBs and absorption computational tests [108]. The authors demonstrated that, at temperature above 450 °C, $Ca(OH)_2$ decomposes into CaO, leading to an oxide/hydroxide blend with a higher specific area and larger diameter, which promotes the interaction between calcium and hydrobromic acid, resulting in brominated salts formation. Furthermore, it has been showed that the metal can interact also with bromophenols, acting directly as debromination agent of organobromine compounds. A more recent work shows that a Br-free oil can be obtained by co-pyrolyzing tetrabromobisphenol A as model compound with calcium hydroxide between 200 and 500 °C. In this system, the sorbent promotes the complete fixation of bromine, while inducing hydrocarbons cracking at the same time [109].

3.3. Ex situ dehalogenation treatments of pyrolysis oil

Post-pyrolysis treatments represent other alternative to obtain a low-halogen content in the liquid fraction. The ex-situ oil upgrading mainly consists of a catalyst/sorbent-mediated process, which allows to customize the liquid fraction properties by simultaneous cracking and dehalogenation. It is usually performed downstream of thermal and/or catalytic pyrolysis.

A number of sorbents and catalysts have been tested in ex-situ dehalogenation treatments, such as heavy metals-based, metal oxides, FCC catalysts and zeolites [110–113]. The latter have been widely studied thanks to the possibility of customizing their adsorbent and catalytic properties by modifying structural and acidic properties. As mentioned above, the zeolite catalytic activity must be considered, since hydrocarbons cracking reactions can lead to the formation of halogenated gases instead of halogen retention. The loading of metals (Mg, Zn, Cu, Ag, Fe) over zeolites can help to overcome this problem by reducing the catalyst acidity and increasing the dehalogenation efficiency through metal halides formation [110].

Hwang et al. tested HY zeolite loaded with different percentage of iron oxide in the catalytic upgrading of chlorinated heavy liquid fraction deriving from pyrolysis of plastic wastes. The authors have demonstrated that Fe-impregnated HY zeolite simultaneously promotes hydrocarbons cracking and Cl-fixation. However, the two effects must be controlled, since a too low iron concentration leads to a high cracking degree, and thus HCl and short Cl-hydrocarbons formation, whilst a too high metal loading brings to a dramatic reduction in zeolite acidity, and then in its cracking activity [114].

Due to the well-known dehalogenation ability of iron-based sorbents, α-Fe_2O_3, γ-Fe_2O_3 and Fe-C composite were tested in the dechlorination of the oil produced from the pyrolysis of a PE, PP and PVC mixture, using a fixed bed reactor at 350 °C[112,113]. The results revealed that iron oxide initially reacts with HCl, being converted into $FeCl_2$. The formed salt is still able to convert organochlorines by reversible interactions, but its cracking activity rapidly decreases, leading to no substantial change in carbon number distribution. Higher dechlorination efficiency and longer sorbent activity can be then reached by continuously removing the generated hydrochloric acid, i.e., by properly modulating the carrier gas flow rate.

The combined effect of metals oxides such as iron, silicon, and aluminium, was studied by Lopez-Urionabarrenechea et al., by testing waste red mud in the dehalogenation of two pyrolysis oils in a stirred autoclave at 325 °C [111]. When compared with a reference thermal experiment, the chlorine retention in the heavy fraction increased by 43-84 % in presence of red mud, together with the gas yield rise, confirming that the zeolitic nature of silica and alumina promotes the cracking, whilst iron mainly acts as sorbent. Furthermore, it was demonstrated that the oil composition plays a key role, since the higher the unsaturated hydrocarbons content, the higher the cracking, then favouring the formation of chlorinated light oil and gases. On the contrary, a high aromatics content-oil undergoes polymerization rather than cracking in these reaction conditions, leading to enhanced heavy fraction yield and dechlorination efficiency (84 %).

The dechlorination mechanism of aromatic and aliphatic hydrocarbons in presence of metal oxides has been recently studied [115]. Using 2-chlorobutane, 2-chloroethylbenzene and chlorobenzene as

model compounds, it has been demonstrated that when an aliphatic hydrogen is adjacent to chlorine, the interaction with metals easily leads to HCl release and olefin formation at relatively low temperature (180 °C). On the contrary, higher temperature is required for the dechlorination of aromatic hydrocarbons (300 °C), as it firstly involves the interaction with a carbocation, which increases the positive charge of the aromatic ring, allowing the negatively charged oxygen of the metal oxide to break the carbon-chlorine bond (Figure 5).

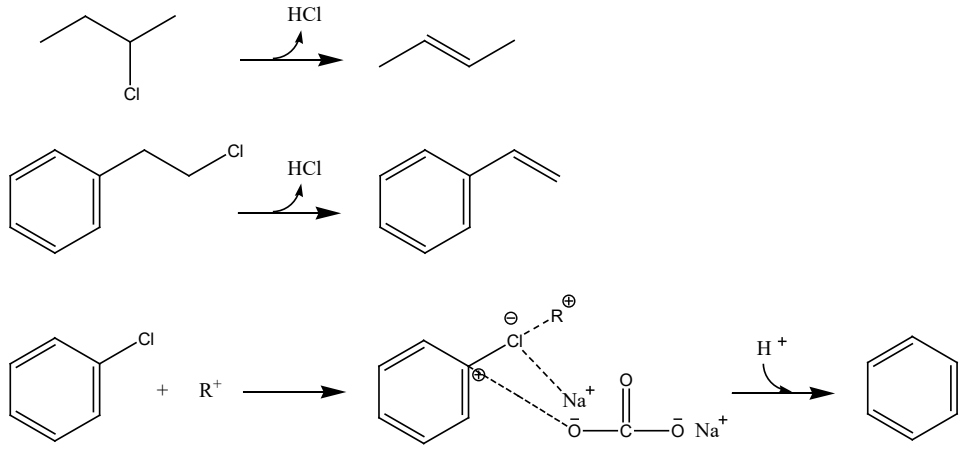

Figure 5. Dechlorination mechanism of aliphatic and aromatic chloro-compounds in presence of metals (adapted from [115]).

4. Co-pyrolysis of plastics with other feedstocks

Usually, plastic waste appears mixed with other types of residues, making necessary their separation by energy intensive and costly methods. However, one interesting alternative is the co-processing of these mixtures, for instance by using them as feedstock for pyrolysis, which may have benefits in terms of improving the economic feasibility of the industrial processes due to the increased plant scale. In addition to that motivation, research on co-pyrolysis has been boosted in recent years due to the synergistic effects that have been observed when plastics are co-processed with other types of waste or even with fossil-based feedstocks (Figure 6) [116–118]. Understanding such synergistic effects are key points for process design minimizing adverse interactions and promoting positive ones.

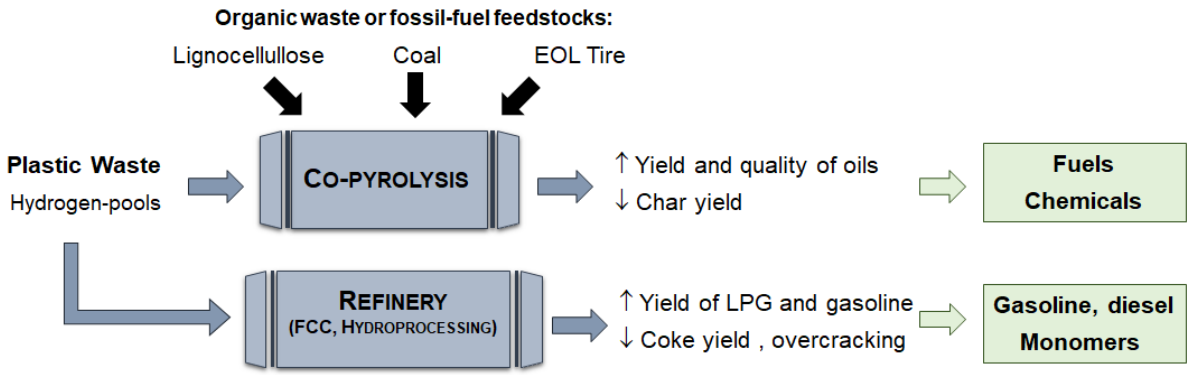

Figure 6. Alternatives and benefits of co-processing plastic waste.

4.1. Types of blending: searching for synergistic effects

Among the mixtures with plastics investigated in co-pyrolysis, those with lignocellulosic biomass have attracted a great attention among the scientific community. Here the interest is mainly to improve the properties of bio-oils from lignocellulose, which are characterized by high oxygen contents, acidity, and viscosity, making them unstable, with low heating values and, therefore, unsuitable to be used as fuels in the transport sector. Plastics are used as hydrogen-pools during the co-pyrolysis with lignocellulosic biomass, leading to an improvement of both the yield and quality of bio-oils. Synergistic effects derive from the interactions between thermal decomposition mechanisms of biomass and synthetic polymers. It has been stated that biomass starts decomposing at lower

temperatures than plastics, hence the radicals so generated promote the further decomposition of plastic polymeric chains, e.g., by β-scission, being then transformed into different alkanes, carbonyl, and hydroxyl groups or even aromatics. In a final reaction stage, biomass and plastic-derived radicals can combine each other and stabilize the molecule structures [119–121]. In addition, these interfering reactions gain predominance as the temperature increases due to a larger formation of free radicals. As a result of such interactions, not only the pyrolysis oil is upgraded in terms of composition and stability, but also other collateral benefits can be achieved, such as lower char formation.

The appearance of beneficial and synergistic effects during the co-pyrolysis of plastics and lignocellulosic biomass is strongly influenced by the nature of both types of waste as well as by the operating conditions. For instance, it has been reported that co-feeding lignocellulose-based waste with PE plastics increases the yield of oil at the expense of char [120,122]. The larger production of oil has been attributed to the hydrogen transfer from PE chain to biomass, enabling both a wider extent of radical-mediated cracking of the synthetic polymer and the stabilization of primary compounds from lignocellulose decomposition. However, this beneficial effect can be lost when the biomass is contaminated with inorganics, mainly metal oxides, as they can catalyze the decomposition of aliphatic hydrocarbons from PE plastics leading to an increase of the char yield [123]. When PVC is used as feedstock, an opposite synergistic behavior than for PE has been reported, with less oil and more char being produced regarding the theoretical values [122,124,125]. Thus, the increase of the solid fraction has been attributed to dehydration of cellulose and inhibition of the pine wood depolymerization caused by the release of HCl from PVC. In addition, it seems that the amount of PVC to be blended with biomass has to be limited to avoid excessive Cl contamination of the oil [126]. Although in a lower extent, co-pyrolysis of plastics has been expanded to other organic waste. This is the case of tires that tend to generate high amounts of solids by pyrolysis, but feeding mixtures with plastics reduces such fraction in favor of oil yields, which also contain progressively larger amounts of lighter compounds as the proportion of plastic is increased [127–129].

The hydrogen donor role of plastics has also been exploited in the co-pyrolysis with low-quality coals [130–132] and other fossil-based feedstocks [133–135]. Thus, blending with waste plastics is considered one of the most promising alternatives for the utilization of low-rank coals in high-quality tar production. For instance, when Pingshuo coal and high-density polyethylene (HDPE) were co-pyrolyzed a large amount of short-chain alkenes (butene and heptadiene) and diphenols were observed, the latest compounds being attributed to the reaction between hydrogen from plastic and the phenoxy group from coal [130]. Pyrolysis of mixtures of low-quality lignite and high-density polyethylene (HDPE) leads to positive effects at temperatures above 450 ºC. Thus, liquid and gas yields, as well as the quality of pyrolytic products, were significantly improved compared with pyrolysis of lignite alone [131]. Regarding oil sludge or heavy petroleum fractions from crude-oil industry, it has been demonstrated that co-feeding plastic waste in the pyrolysis units helps to improve the quantity and quality of pyrolytic oils, which become lighter and with larger proportions of paraffinic hydrocarbons [133,134]. In fact, the oil industry could play a key role in the plastic waste management chain as plastics can be blended with several refinery streams without severe changes in their production strategies, provided they are free of contaminants like halogen-containing species.

4.2. Catalytic co-pyrolysis

Although co-pyrolysis of plastics and other types of waste has proven to be an effective strategy to improve the performance and properties of pyrolysis oils, their composition and physicochemical properties, such as density and viscosity, are still too far from the specifications to be marketed or blended in refineries. The integration of the co-feeding of waste with catalysts, that is, catalytic co-pyrolysis, could bring the process closer to industrial scale applications.

Blends of lignocellulosic biomass with synthetic polymers (e.g., PE, PP, PS, etc.) and zeolite-based catalysts is by far the most studied tandem in catalytic co-pyrolysis research [136–138]. Nowadays, it is well known that the combination of acidic zeolites and hydrogen-rich feedstocks result in significant improvements in the yield of petrochemicals (aromatics and olefins) from pyrolysis of biomass. Due to their unique acidity and microporous (shape-selectivity) properties, zeolites are excellent catalysts

to induce, not only cracking, but also other desired reactions, such as decarboxylation, dehydration, isomerization, and aromatization, resulting in a promotion of aromatics and furans from biomass. If plastics are co-fed, zeolites decompose them into light olefins and promote their further combination with biomass-derived furans through Diels-Alder reactions followed by dehydration to yield more aromatic hydrocarbons. In addition, the plastic-derived olefins could individually be converted into aromatics by cyclization, aromatization, and oligomerization reactions. An overall reaction network for the catalytic co-pyrolysis of lignocellulose and plastics was illustrated by Zhang et al.[139] . Finally, in their role as hydrogen-donors during cracking, plastics can mitigate (but not eliminate) the formation of coke on the catalyst surface. It has been proposed that hydrogen from plastics reacts with phenolic compounds derived from lignin causing their stabilization and, therefore, preventing their polymerization to coke [139,140].

Most of the research in this area has been carried out with ZSM-5 zeolite since its strong acidity, microporosity, relatively high surface area and stability make this material an efficient catalyst to produce both olefins and aromatic hydrocarbons [139,141,142]. Nevertheless, despite the excellent catalytic properties of ZSM-5, there is still room to improve its performance and, consequently, achieve larger yields of high-quality oils. Higher selectivity to valuable petrochemicals, lower coke formation and higher resistance to chemical deactivation by heteroatoms from waste, are the main challenges nowadays. Different strategies have been proposed for the modification of ZSM-5 zeolite based on the incorporation of additional active phases with hydrogen transfer capacity, introduction of mesoporosity (hierarchical zeolites) and/or modification of acidity [143]. On the other hand, in addition to zeolites, low-cost catalysts, such as activated carbons [144] and red mud [145] are also being explored in co-pyrolysis processes to improve their economic feasibility. Table 2 summarizes the above commented main results of catalytic co-pyrolysis

Table 2. Main results on catalytic co-pyrolysis of plastic waste.

Blending & Catalytic system	Highlights	Ref.
• Biomass: Douglas fir (DF) sawdust; Cellulose • Plastic: LDPE • Catalyst: ZSM-5 • Reactor: Ex-situ MW-induced pyrolysis system	• Adding LDPE to biomass: higher oil carbon yield while less char and coke. • Optimized T and plastic/DF ratio: liquid carbon yield of 40.54% with compositions in the jet fuel range. • LDPE-derived olefins hinder the formation of polyaromatics from cellulose by suppressing polymerization reactions.	139,142
• Biomass: Cellulose, xylan and milled wood lignin • Plastic: PE • Catalyst: ZSM-5 • Reactor: Tandem micropirolyzer	• Thermal co-pyrolysis: increased light oxygenates from carbohydrates, more phenolic monomers from lignin and shorter olefins from PE. • Catalytic co-pyrolysis: synergetic effect towards aromatic HCs production (26, 30, 50 % higher than theoretical in blendings with cellulose, xylan and lignin, respectively).	140
• Real MSW: Mix of PP, LDPE, HDPE, newspaper, cardboard and others. • Catalyst: Zeolite (ZSM-5, SAPO-11)-based composites • Reactor: Batch and continuous tubular reactors	• Zeolite-based catalysts promote cracking of polyaromatics and aromatization reactions. • Monoaromatics concentration increases from 6.1 (thermal pyrolysis) up to 18.2 % with ZSM-5-based catalyst.	141
• Biomass: Douglas fir (DF) sawdust. • Plastic: LDPE • Catalyst: Hierarchical ZSM-5 vs conventional ZSM-5 • Reactor: Fixed-bed reactor	Introduction of mesoporosity by alkaline treatment leads to: • Higher selectivity to monoaromatics (18 vs 32 % in parent and hierarchical ZSM-5, respectively) • Coke formation inhibition.	146
• Biomass: Sawdust. • Plastic: Real MSW (mix of food waste, PVC and lignocellulose) • Catalyst: Multilamellar MFI nanosheets vs conventional ZSM-5 • Reactor: Micropyrolyzer	Introduction of mesoporosity and changing the acidity through lamellar morphology leads to: • Higher yield of mono and polyaromatics. • Lower yield of oxygenated compounds (14.82 vs 3.37 %)	147
• Biomass: Wheat straw • Plastic: HDPE	Modifying ZSM-5 by metal impregnation leads to: • Higher organic oil yield mainly due to more aliphatics and aromatics.	148

• Catalyst: Metal (Mn, Ni, Zn) modified-ZSM-5 • Reactor: Fixed-bed reactor	• Proportion of aromatics directly related to the total acidity of catalysts (larger total acidity than parent ZSM-5 up to 5% metal loading) • Metal incorporation promoted deoxygenation reactions, being particularly boosted with 5% Ni loading.	
• Biomass: Douglas fir sawdust pellets • Plastic: LDPE pellets • Catalyst: Activated carbon modified with Fe • Reactor: Fixed-bed reactor	• Adding LDPE to biomass: thermal synergy decreasing the formation of char. • Strong promotion of aromatics and yield of phenols (3.0%) much lower than the theoretical value (38.8%).	144

5. Multi-scale modelling and process analysis

5.1. Kinetic modelling of plastic pyrolysis

Lumped kinetic models are typically applied for plastics pyrolysis, calculating the solid feedstock conversion (α) as a function of the temperature through an Arrhenius-type power law. Table S1 in the Supporting Information reports the most common kinetic models, whilst Table S2 summarizes the main results from kinetic investigations of plastic pyrolysis available in the open literature [149–159]. As a general trend, polyethylene presents greater activation energy than polypropylene and polystyrene. Three different studies ([149,150,152]) identified the reaction model R2 (contracting sphere) and R3 (contracting cylinder) as the best fitting methods for PE and PP thermal pyrolysis, respectively.

To increase the model accuracy, some multi-equation models (semi-lumped) have been also proposed [160–162], where thermal pyrolysis is described through the evolution of macro-categories of intermediates/products, such as gas, liquid, char, waxes, and aromatics evolving in a combination of parallel and series of decomposition reactions.

Focusing on thermal decomposition of PE, PP and PS, each elementary step of degradation mechanism is characterized by specific kinetic parameters [19,20]. Therefore, the mass balance for each involved radical and stable species should be solved to completely describe the time evolution of species population. Paraffinic, olefinic and diolefinic species (molecules/radicals) can be identified and tracked. All the mass balances thus can form a set with hundreds thousand ordinary differential equations (ODEs), leading to a time-consuming procedure for numerical resolution. Some techniques, as steady-state approximations, discrete section and method of moments have been proposed to reduce the calculation effort [19].

The methodology for kinetic assessment of catalytic pyrolysis via lumped models follows the same approach described for thermal decomposition, hence kinetic parameters can be evaluated for different solid catalysts and polymers[46,163–172]. As a general trend (see Table S3 in the Supporting Information), catalyst causes a reduction of the activation energy with respect to thermal pyrolysis and modifies the values of the kinetic parameters fitted since the catalyst presence induces important

changes in the reaction mechanisms. On the other hand, experimental validation is done via reactant conversion and (apparent) kinetic parameters are expected (both for thermal and catalytic pyrolysis). Since real decomposition mechanism includes different both intermediate/products and reaction pathways as a function of temperature, kinetic parameters could be rather inconsistent. This a reasonable consequence of the use of a unique kinetic equation to describe a complex multi-step phenomenon (like carbenium ion mechanism, as previously pointed out).

Some authors have proposed semi-lumped reaction schemes accounting for the main steps of the decomposition reaction pathways, lumping the pyrolysis products into main groups (as shown in Figure 7). Huang et al., [173] proposed a kinetic model based on the carbenium ion mechanism already described for polymers cracking over acidic zeolitic (USY, ZSM-5, Mordenite) and non-zeolitic (MCM-41, ASA) catalysts. According to this model, the fed solid polymer instantaneously melts and forms a polymer/catalyst complex. Intermediates like long-chain olefins and precursors for carbenium ions are formed. During this phase large alkanes may be generated. Then, further reactions could lead to the formation of shorter chain olefins in equilibrium with surface carbenium ions, as well as alkanes, BTX and coke. For each lumped step, the reaction rate includes an activity decay term accounting for catalyst deactivation, expressed as an exponential function of produced coke. The simultaneous reactions are simple first-order expressions. The generation of intermediates like long-chain olefins is faster (especially for zeolites) than the production of paraffinic, BTX and coke lumps. Zeolites seems to be more effective in converting polymers to intermediates of volatile precursors than amorphous catalysts.

Till et al., [174] proposed a reaction network with ten irreversible reactions between six lumps. Plastic feedstock firstly decomposes, forming a cracked lighter intermediate that may subsequently undergo decomposition into heavy/light liquid, gas, and coke (which can be additionally produced by further reaction of liquids). Each lumped group includes several species/molecules; light and heavy liquids include species with carbon atom number in the range 6-15 and 16-30, respectively. Plastic feedstock, cracked intermediate, and coke are treated as quasi-solid species, while the other groups are

considered in fluid status, without mass transfer limitations between the two phases. Reaction rates are considered to follow first-order Arrhenius-type equations, and stoichiometric matrix enables the calculation of production/consumption rates.

In summary, for catalytic plastics pyrolysis a semi-lumped reaction scheme (instead of a fully mechanistic approach) probably represents a good trade-off between precision of products distribution and computational cost when reactor modelling and sizing is carried out.

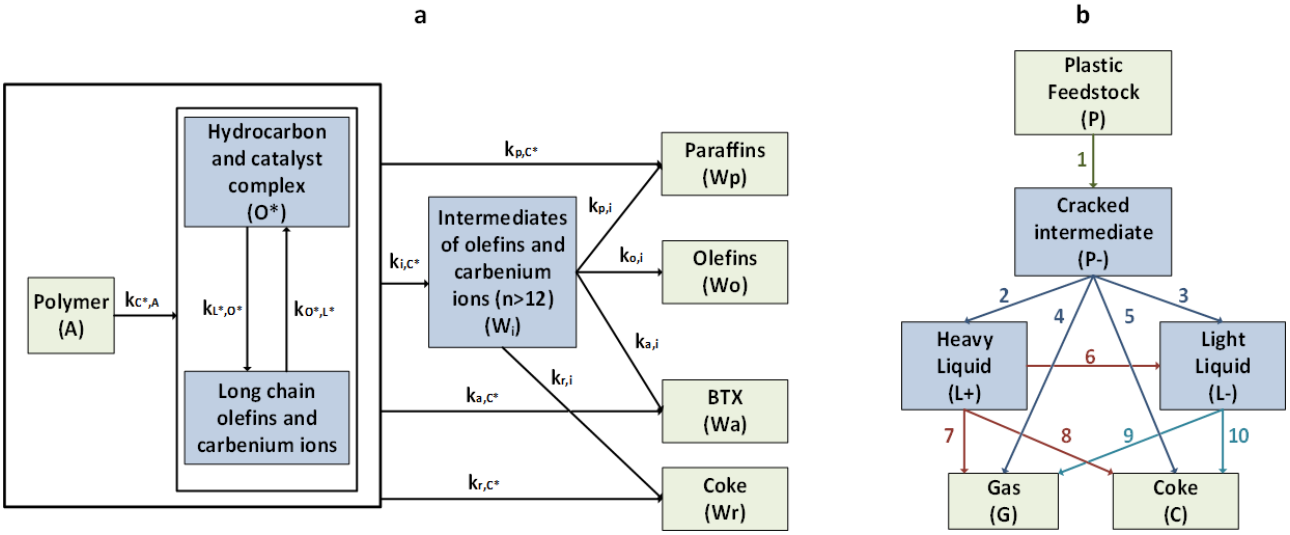

Figure 7. Semi-lumped kinetic schemes proposed for catalytic pyrolysis of a) PE/PP/PS mixture over acidic cracking catalysts (adapted from [173]) and b) PE/PP waste mixture over zeolites (adapted from [174]).

5.2. Reactor features

Table 3 summarizes benefits and challenges for the main classes of reactors employed to perform plastics pyrolysis processes. Additional details and description can be found for fixed bed [126], rotary kiln [126], auger [175], fluidized-bed [176] and spouted-bed reactors [126]. Rotary kiln and auger/screw types are usually employed in thermal pyrolysis [177], whilst fixed bed, batch/semi-batch and fluidized/spouted bed can be operated with or without a solid catalyst.

The choice of the most suitable reactor for pyrolysis at industrial scale strongly depends on the process that is carried out. For slow thermal pyrolysis, rotary kiln, auger and semi-batch reactors probably represent the best options, since they are designed to ensure long residence time. If fast (thermal or

catalytic) pyrolysis is targeted, fluidized bed reactor is the most convenient type also due to the scale-up ease. In the case of fast thermal pyrolysis in fluidized bed reactors, the heat needed for the endothermal decomposition can be provided by using a solid inert in contact with the feedstock. When catalytic pyrolysis in a fluidized bed is carried out, a separated section for catalyst regeneration should be considered. If this operation is exothermal, regenerated catalyst can also represent the heat carrier providing at least part of the required thermal energy.

Table 3. Main reactor types involved in pyrolysis.

Reactor type	Advantages	Drawbacks
Fixed bed	• Low cost • simple design	• Difficulties in uniform heating at commercial scale. • Poor catalyst-particle contact when catalytic pyrolysis is carried out.
Batch/semi-batch	• Operating condition control • High conversion	• Char/solid residues removal. • Non uniformity of products (Variability of products composition from batch to batch) • In catalytic pyrolysis case catalyst regeneration is not straightforward.
Rotary kiln	• Simple feedstock pre-treatment • Good solid mixing	• Heat transfer limitation (if compared with fluidized bed). • High residence time.
Auger/screw reactor	• Continuous operation • Good residence time control • Good scalability and portability	• Short residence time hard to achieve. • High char yield. • High maintenance costs.
Fluidized bed	• Process flexibility • Easy scale-up • Good heat/mass transfer • Limited maintenance costs	• Only for fast pyrolysis (low residence time). • Attrition (especially in presence of a catalyst). • If a catalyst is employed, regeneration. • Char separation
Spouted bed	• Suitable for pyrolysis of waste materials • Continuous operation • High heat/mass transfer	• Small particles required. • Scale-up is not easy. • Catalyst circulation (if present). • Attrition (but lower than fluidized bed).

Computational fluid dynamic (CFD) models have been developed to analyze pyrolysis reactors performance, using a combination of Eulerian and Lagrangian approaches to describe the evolution of both fluid phase (solid and/or liquid) and particles (solid, catalyst, molten plastic).

Xiong et al. [178], overviewed possible models for solid feedstock pyrolysis at reactor scale and CFD modelling of coupled hydrodynamics and kinetics has been grouped into three main categories according to reactor characteristics: (i) porous media modelling (PMM) for fixed-bed pyrolysis, (ii) multifluid modelling (MFM) of fluidized bed pyrolysis and (iii) discrete particle modelling (DPM).

Porous media models (PMM) can be used for fixed bed modelling, where governing equations (mass, momentum, energy, and species balance, respectively) are formulated for gas phase. Mass, energy, and species conservation equations for solid bed can be formulated without convective term since solids remain stationary. Intraparticle mass and heat transfer can be coupled with PMM when they are not negligible. Zavala-Gutiérrez et al. [179] developed a model for catalytic pyrolysis of HDPE in a fixed-bed reactor assuming tubular plug-flow. Isothermal operation was considered, as well as the absence of transport limitations. A pseudo-mechanistic kinetic scheme was implemented, leading to a set of 20000-50000 ODEs that must be simultaneously solved.

Fluidized-bed pyrolysis reactors behavior is usually simulated through multifluid models (MFM), where the involved phases (solid and fluid) are modelled as interpenetrating continua. Conservation equations for gas-solid transfer is modelled by using interphase coefficients (e.g., drag coefficient for momentum equation). Contrarily to PMM, the solid phase is not static and thus a solid stress term must be included through the kinetic theory of granular flow, where the so-called granular temperature is defined to obtain pseudo-solid transport properties (e.g., viscosity) [178]. Niksiar and Sohrabi developed a mathematical model to simulate unsteady behavior of a conical spouted bed reactor for pyrolysis of waste plastics. Conservation equations have been written for the three main zones in which the domain have been divided, i.e., spout, annulus, and fountain core [180].

Each solid particle can be tracked individually (Lagrangian approach) and treated as a discrete object in the discrete particle model (DPM). Interactions between solid particles are reproduced through

collision models. In DPM the computational cost is mainly devoted to solid phase equations and is thus almost proportional to the number of solid particles. On the other hand, if compared to MFM, the accuracy of DPM is greater. Nevertheless, due to computational effort reasons, simulation of commercial scale reactors through DPM is not feasible because of the huge number of solid particles that must be simultaneously modelled.

A two-dimensional model (built on ANSYS Fluent) was recently reported to simulate catalytic pyrolysis of HDPE within a fluidized-bed reactor by using ZSM-5 [181]. A semi-lumped scheme was considered for the pyrolysis kinetics. Navier-Stokes equations were solved throughout the domain, while heat and mass transfer were accounted for via Reynolds, Sherwood and Nusselt dimensionless groups. Gidaspow's approach was used for the fluid–solid exchange. The k-epsilon model was employed for turbulence. Sensitivity analysis was carried out to evaluate the effect of temperature and space velocity on conversion and product distribution. According to the presented results, the reactor fed with a flux of 1 kg m^{-2} s^{-1} at 500 °C showed the best gasoline production (≈ 31 wt.-%) and the lowest energy consumption, while simulations at 400 °C showed the best liquid-to-gas ratio.

Gala et al. [182], simulated (via CFD model built in Comsol Multiphysics) a reactor at pilot scale (30 kg/h) for *ex-situ* catalytic hydrotreatment of oil from LDPE decomposition. A multi-tubular, fixed-bed, reactor equipped with 37 tubes (filled with catalyst) is fed with a hydrocarbon mixture ranging between C_5 and C_{32}. A thermal oil (circulating in the shell) is used as coolant to moderate the temperature rise throughout the tube due to exothermal reactions occurring. Navier-Stokes equations with the Brickman correction for the catalytic porous medium were solved. Sensitivities has been carried out to evaluate the effect of spatial time, coolant flow and H_2/pyrolysis oil ratio. A complete olefin conversion into paraffins was estimated to be achieved after 1000 mm from the inlet.

Numerical modelling thus represents a useful tool for the design of pyrolysis and catalytic ex-situ reactors at pilot/full scale, driving the choice of key parameters like size, temperature, space velocity and catalyst-to-feedstock ratio. In case of catalytic pyrolysis, catalyst deactivation kinetics may be

implemented into the model to assess the performance time evolution or the design of regeneration unit (when fluidized reactor is involved).

5.3. Pyrolysis at process scale

As illustrated in Figure 8, a typical plant/process for plastics pyrolysis involves feedstock pre-treatment, solid displacement, heating systems, pyrolysis reactor, product upgrading and separation and auxiliary sections (compression, recirculation, heat recovery, heat exchangers). Feedstock generally requires pre-treatment like mechanical particle size reduction prior to feeding into a pyrolysis reactor [183]. Separation of plastics from metals and residues as well as feedstock drying should be carried out. Special attention should be paid to dehalogenation processes that can eventually be carried out before pyrolysis to avoid the formation of pollutant and corrosive halogenated compounds as HCl.

Before thermal decomposition, feedstock must be melted and heated up to the decomposition temperature whatever thermal or thermo-catalytic decomposition can be carried out. Non-condensable gases and char exiting the pyrolysis reactor can be fully/partly burned to provide the necessary process heat for feedstock decomposition and steam generation. After pyrolysis, the produced vapor enters a solid separation section, being then sent to a series of heat exchangers and separators operating at decreasing temperature (from ≈ 400 °C to ≈ 25 °C) where the condensable fraction is collected. As above indicated, a catalyst can be employed to carry out *in-situ* or *ex-situ* upgrading of the oil phase. Further conversion may be required if the final product should meet prescriptions to be considered as a substitute of fossil-derived fuels as gasoline, naphtha, or diesel. One or more steps of upgrading could be required depending on the quality of the original raw stream [184,185].

Catalytic cracking over porous acid solids (mainly zeolites) allows optimizing the mixture composition, especially when the final product is destinated to automotive fuels or petrochemical industry [186–188]. Hydrotreating is commonly used in the oil industry to selectively remove heteroatoms like S, N, Cl and O that may be present in some plastic pyrolysis oils [189]. It is carried out through a

hydrogen-rich stream in the presence of a solid catalyst (e.g., Ni-Mo/Al_2O_3) at high pressure (20-200 atm) and temperature usually in the range 300-400 °C [183,186,190]. Trickle-bed reactors are commonly used in hydrotreating. To preserve the most active catalyst from poisoning and deactivation, a common industrial strategy is to place different catalyst beds in series, with increasing order of activity [190]. Hydrotreating can be followed by hydrocracking to break down heavy molecules into shorter chains in presence of hydrogen [190]. Hydrocracking is usually carried out at a pressure up to 70 atm and at a temperature in the range of 300-400 °C [191,192]. Thus, catalysts with Ni on different acidic supports like H-Beta, SAPO-11 and HMCM-41 have been investigated for the hydrocracking of polyolefins pyrolysis waxes. [182]Via hydrocracking of plastics pyrolysis oil, the production of a good quality naphtha can be achieved [191]. Nevertheless, one of the main obstacles in implementing hydrotreatment and hydrocracking is the cost of hydrogen. Another challenge affecting costs and commercial viability is catalyst poisoning effect when hydrocracking of PVC-derived products is carried out [193].

On the other hand, among the possible ways to upgrade the decomposition products, pyrolysis with in-line steam reforming is reported when the main desired product is hydrogen [193]. Reforming step occurs in a second reactor connected with the pyrolyzer and it is commonly carried out at a temperature range of 600-800 °C and in presence of a Ni-based catalyst, which should be preserved from impurities that could deactivate it [194]. Steam reforming reactions are endothermal and convert hydrocarbons (and oxygenates, when present) into H_2 and CO. Fixed bed reactors are usually considered for steam reforming, even though - with some pyrolysis vapor compositions - it may be affected by coke deposition on the catalyst surface, leading to deactivation and bed blockage [194]. H_2 potential production strongly depends on the raw plastic material and thus on the composition of pyrolysis vapors. When pure hydrogen production is required, the gaseous stream should be sent to a water gas shift section to convert CO into CO_2, which can be more easily separated in a subsequent pressure/temperature swing adsorption (PSA/TSA) unit.

Finally, treated pyrolysis products can be selectively separated and stored for direct use or further refining through fractional condensation, scrubbing, and distillation unit [185,186,195,196].

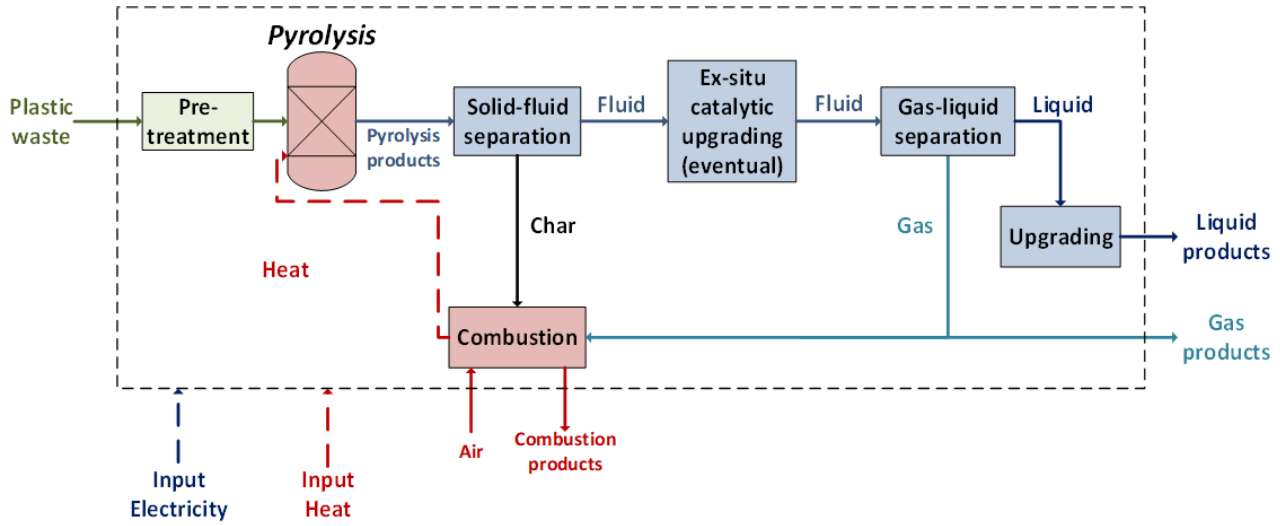

Figure 8. Schematic of a typical plastics waste pyrolysis process.

Some studies available in the open literature have addressed the process modelling and techno-economic assessment of commercial-scale waste plastics pyrolysis plants [196–201]. Aspen Plus™ is often used as simulation software for mass and energy balances of the single units and for the whole system [202–205]. Economic assessment is generally based on discounted cash flow analysis. This approach is related to the calculation of the net present value (NPV).

Table 4 presents an overview of economic results from articles available in the open literature dealing with techno-economic assessment of waste plastics pyrolysis processes. Some works [197,199] carried out a cost analysis of fuel substitute production via catalytic and thermal pyrolysis of plastic waste, respectively. Both articles focused on processes involving a fluidized bed reactor and analyzed the effect of scale-up on the production cost. A comparison of the results from these two works indicates that the economic feasibility is achieved with a larger plant size, mainly because of higher investment cost at similar scale. In general, the cost analysis and the economic feasibility estimation are affected by several factors like the involved cost functions (and the uncertainty in capital cost estimation), the scale factors (e.g., Lang factor or capital cost exponent), the composition of inlet plastic waste and the desired final product (e.g., a specific olefin or a hydrocarbon mixture). The last aspect strongly affects the process configuration, the conceptual design, and the required equipment, leading to

different capital cost expenditure. The chosen final product has an impact on the economic feasibility since it should be compared with the corresponding current market price, which may fluctuate over time. Furthermore, other parameters that may affect economic analysis are the feedstock and external energy cost, as well as financial assumptions like discount rate and lifetime. Sensitivity analyses should be carried out to evaluate their impact on process economics.

The recently published techno-economic assessments agree in concluding that scale-up at full industrial size is essential to ensure the economic feasibility of plastics pyrolysis, making the production cost of investigated process comparable with the corresponding market price. Even though the size allowing the economic profitability differs between the studies, it generally lies in the range 10-100 kt of fed plastics per year. When ethylene monomer recovery was investigated a plant of about 150 kt/y was considered, leading to a production cost of ≈ 0.39 €/kg, considerably lower than that of conventional route (≈ 0.83 €/kg) [200]. This means that even a lower plastics input should ensure the economic feasibility. If the target is pyrolysis oil production as substitute of hydrocarbon mixtures, a size of about 10 kt per year has been reported to achieve the economic profitability of plastics pyrolysis [199], although a recent work provided a less optimistic evaluation, estimating a break-even size of about 100 kt/year [203].

Table 4. Overview of techno-economic assessments for plastics pyrolysis processes. ROR stays for rate of return. TCI is total investment cost.

Brief process description	Main economic results	Ref.
Catalytic fluidized bed reactor Small size: 10 kt/y Medium size: 60 kt/y Large size: 120 kt/y	Small scale. ROR: 4.17%; payback: 24 y Medium scale. ROR: 23.76%; payback: 4.5 y Large scale. ROR: 35. 69%; payback: 1.5 y	197
Fluidized bed reactor 0.1 t/h (base case) Scaled-up cases: 1; 10 and 100 t/h	0.1 t/h. TCI: 0.99 M£; product cost: 0.87 £/kg 1 t/h. TCI: 3.06 M£; product cost: 0.26 £/kg 10 t/h. TCI: 9.35 M£; product cost: 0.05 £/kg 100 t/h. TCI: 56.77 M£; product cost: 0.03 £/kg	199
Furnace pyrolysis reactor fed with PE (18.9 t/h) Main products: ethylene, methane, propylene, butene, benzene	Total installation cost: 29.9 M€ Ethylene production cost: 0.386 €/kg	200
Molten salt pyrolysis reactor. Mixed plastic waste.	4 kt/y. TCI: 3.63 M$; IRR: 9.6 % 8 kt/y. TCI: 4.41 M$; IRR: 27.1 % 16 kt/y. TCI: 6.44 M$; IRR: 37.1 %	202
Pyrolysis of mixed (PE+PP) plastics waste (base case: 84 kt/y) Produced oil: 37 kt/y	Total investment cost: 40 M$ Minimum selling price for pyrolysis oil: 600 $/t	203

6. Conclusions and perspectives

Pyrolysis is one of the most promising technologies to deal with the enormous volume of plastic waste currently generated. Compared to traditional management alternatives, like incineration or landfilling, those plastic waste non-suitable for mechanical recycling could be valorized into chemicals or high-quality liquid fuels by pyrolysis, contributing to the objectives of circular economy. However, current industrial plants apply thermal pyrolysis treatments to a limited range of waste plastics, since the presence of pollutants and halogens in the composition of many raw materials pose technological barriers that still need to be resolved.

Catalytic pyrolysis is expected to emerge at industrial scale as the next generation of thermochemical processes for the conversion of plastic waste into more valuable products than those coming from thermal pyrolysis. Among the challenges to be faced, catalyst deactivation and regeneration are relevant issues due to the possible presence of catalyst poisons in the plastic waste feedstock. In addition, the development of specific catalysts with enhanced accessibility is required to deal with the bulky compounds present or derived from plastic waste. In this way, special attention should be paid to confinement effects around the acid sites and the hierarchy and interconnectivity of the porous structure, since they affect meaningfully to both the conversion and product distribution as well as to the catalyst deactivation by coke deposition.

The presence of halogens in plastic waste represents a strong limiting factor for the scale-up of the pyrolysis processes due to their relevant negative impacts according to health and environmental criteria, as well as regarding the possible corrosion of the industrial plants. In recent years, significant progresses have been achieved on both ex-situ and in-situ dechlorination/debromination treatments. Future efforts should be devoted to the development of single-step processes, based on the use of sorbent/catalyst composites able to direct the pyrolysis products distribution while simultaneously removing different halogens, without suffering poisoning and/or deactivation. This would allow to reduce limitations and costs related to the multi-step pyrolysis processes.

The pyrolysis plants of the future must be versatile and robust to respond to the heterogeneity of the waste to be processed: mixture of plastics or even containing other organic wastes and/or biomass residues. In this way, the oil industry should play a leading role in the chain of plastic waste upcycling since the pyrolysis oil can be blended with several refinery streams. Moreover, with proper research and understanding of the interactions that can occur between these feedstocks and even with catalysts, beneficial synergistic effects can be identified.

Kinetic analysis is crucial for multi-scale modelling of thermal and/or catalytic plastics pyrolysis, allowing the estimation of products distribution. Lumped, semi-lumped and mechanistic approaches have been reported, with the latter ones providing a more precise estimation of pyrolysis products, even though with a greater computational cost. Future works should be focused on the investigation of techniques reducing the numerical effort still guaranteeing an acceptable precision. These kinetic models are needed to be coupled with mass, energy and momentum balances at reactor scale providing a proper estimation of the behavior of commercial-scale pyrolysis devices. The choice of reactor type depends on the feedstock, desired products, operating conditions and size, as well as on the presence of a solid catalyst to carry out catalytic pyrolysis. According to economic criteria, thermal pyrolysis systems require lower investment costs than catalytic processes, although the latter leads to more valuable upgraded products. Thus, catalytic pyrolysis may drive the process towards components that could be used as monomers or raw chemicals, thus enhancing the plastic waste circularity.

In spite of the great number of literature references produced in the past years on plastic pyrolysis, some aspects need to be further covered for accelerating the industrial implementation of these processes, such as: tests with real plastic waste addressing the problems derived from their complexity, enhanced focus on the performance of ex-situ catalytic pyrolysis systems, better understanding of the halogen fate during pyrolysis and deeper exploitation of the co-pyrolysis of waste plastics with other materials.

References

1 United Nations, *Plastic Waste. Background Report.*, 2020.

2 Statista, *Plastic waste in Europe*, 2021.

3 D. K. Sharma, S. Bapat, W. F. Brandes, E. Rice and M. J. Castaldi, *Waste Biomass Valorization*, 2019, **10**, 1355–1363.

4 J. Aguado and D. P. Serrano, *Feedstock Recycling of Plastic Wastes*, The Royal Society of Chemistry, 1999.

5 W. Kaminsky, *J Anal Appl Pyrolysis*, 1985, **8**, 439–448.

6 J. Aguado, D. P. Serrano and J. M. Escola, *Ind Eng Chem Res*, 2008, **47**, 7982–7992.

7 S. M. Al-Salem, A. Antelava, A. Constantinou, G. Manos and A. Dutta, *J Environ Manage*, 2017, **197**, 177–198.

8 S. D. Anuar Sharuddin, F. Abnisa, W. M. A. Wan Daud and M. K. Aroua, *Energy Convers Manag*, 2016, **115**, 308–326.

9 R. Miandad, M. A. Barakat, A. S. Aburiazaiza, M. Rehan and A. S. Nizami, *Process Safety and Environmental Protection*, 2016, **102**, 822–838.

10 D. P. Serrano, J. Aguado and J. M. Escola, *ACS Catal*, 2012, **2**, 1924–1941.

11 A. Marcilla, M. I. Beltrán and R. Navarro, *J Anal Appl Pyrolysis*, 2009, **86**, 14–21.

12 E. A. Williams and P. T. Williams, *J Anal Appl Pyrolysis*, 1997, **40–41**, 347–363.

13 J. Joo, E. E. Kwon and J. Lee, *Environmental Pollution*, 2021, **287**, 117621.

14 M. S. Qureshi, A. Oasmaa, H. Pihkola, I. Deviatkin, A. Tenhunen, J. Mannila, H. Minkkinen, M. Pohjakallio and J. Laine-Ylijoki, *J Anal Appl Pyrolysis*, 2020, **152**, 104804.

15 V. K. Soni, G. Singh, B. K. Vijayan, A. Chopra, G. S. Kapur and S. S. V. Ramakumar, *Energy and Fuels*, 2021, **35**, 12763–12808.

16 R. Mishra, A. Kumar, E. Singh and S. Kumar, *ACS Sustain Chem Eng*, 2023, **11**, 2033–2049.

17 T. Xayachak, N. Haque, R. Parthasarathy, S. King, N. Emami, D. Lau and B. K. Pramanik, *J Environ Chem Eng*, 2022, **10**, 108865.

18 D. P. Serrano, J. Aguado, J. M. Escola and E. Garagorri, *J Anal Appl Pyrolysis*, 2001, **58–59**, 789–801.

19 A. Marongiu, T. Faravelli and E. Ranzi, *J Anal Appl Pyrolysis*, 2007, **78**, 343–362.

20 E. Ranzi, T. Faravelli and F. Manenti, *Advances in Chemical Engineering*, 2016, **49**, 1–94.

21 T. P. Wampler, *J Anal Appl Pyrolysis*, 1989, **15**, 187–195.

22 J. M. Escola, J. Aguado, D. P. Serrano and L. Briones, *J Mater Cycles Waste Manag*, 2012, **14**, 286–293.

23 W. Kaminsky, M. Predel and A. Sadiki, *Polym Degrad Stab*, 2004, **85**, 1045–1050.

24 Z. Zhang, T. Hirose, S. Nishio, Y. Morioka, N. Azuma, A. Ueno, H. Ohkita and M. Okada, *Ind Eng Chem Res*, 1995, **34**, 4514–4519.

25 P. T. Williams and E. A. Williams, *Journal of the Institute of Energy*, 1998, **71**, 81–93.

26 M. S. Abbas-Abadi, Y. Ureel, A. Eschenbacher, F. H. Vermeire, R. J. Varghese, J. Oenema, G. D. Stefanidis and K. M. Van Geem, *Prog Energy Combust Sci*, 2023, **96**, 101046.

27 N. Miskolczi, in *Feedstock Recycling and Pyrolysis of Waste Plastics: Converting Waste Plastics into Diesel and Other Fuels*, 2006, pp. 225–247.

28 G. Elordi, M. Olazar, M. Artetxe, P. Castaño and J. Bilbao, *Appl Catal A Gen*, 2012, **415–416**, 89–95.

29 G. Elordi, M. Olazar, G. Lopez, M. Artetxe and J. Bilbao, *Ind Eng Chem Res*, 2011, **50**, 6061–6070.

30 G. Elordi, M. Olazar, G. Lopez, P. Castaño and J. Bilbao, *Appl Catal B*, 2011, **102**, 224–231.

31 G. Manos, A. Garforth and J. Dwyer, *Ind Eng Chem Res*, 2000, **39**, 1203–1208.

32 C. Covarrubias, F. Gracia and H. Palza, *Appl Catal A Gen*, 2010, **384**, 186–191.

33 G. Manos, A. Garforth and J. Dwyer, *Ind Eng Chem Res*, 2000, **39**, 1198–1202.

34 A. Marcilla, M. I. Beltrán and R. Navarro, *Appl Catal B*, 2009, **86**, 78–86.

35 S. C. Cardona and A. Corma, *Appl Catal B*, 2000, **25**, 151–162.

36 S. C. Cardona and A. Corma, *Catal Today*, 2002, **75**, 239–246.

37 A. A. Garforth, Y. H. Lin, P. N. Sharratt and J. Dwyer, *Appl Catal A Gen*, 1998, **169**, 331–342.

38 J. Aguado, D. P. Serrano, M. D. Romero and J. M. Escola, *Chemical Communications*, 1996, 725–726.

39 M. Artetxe, G. Lopez, M. Amutio, G. Elordi, J. Bilbao and M. Olazar, *Chemical Engineering Journal*, 2012, **207–208**, 27–34.

40 R. Bagri and P. T. Williams, *J Anal Appl Pyrolysis*, 2002, **63**, 29–41.

41 J. Aguado, D. P. Serrano, G. San Miguel, M. C. Castro and S. Madrid, *J Anal Appl Pyrolysis*, 2007, **79**, 415–423.

42 M. del Remedio Hernández, Á. N. García and A. Marcilla, *J Anal Appl Pyrolysis*, 2007, **78**, 272–281.

43 D. P. Serrano, J. Aguado, J. M. Escola, J. M. Rodríguez and G. San Miguel, *J Anal Appl Pyrolysis*, 2005, **74**, 370–378.

44 P. L. Beltrame, P. Carniti, G. Audisio and F. Bertini, *Polym Degrad Stab*, 1989, **26**, 209–220.

45 J. Aguado, D. P. Serrano, J. M. Escola, E. Garagorri and J. A. Fernández, *Polym Degrad Stab*, 2000, **69**, 11–16.

46 X. Tian, Z. Zeng, Z. Liu, L. Dai, J. Xu, X. Yang, L. Yue, Y. Liu, R. Ruan and Y. Wang, *J Clean Prod*, 2022, **358**, 131989.

47 G. De La Puente, C. Klocker and U. Sedran, *Appl Catal B*, 2002, **36**, 279–285.

48 A. Peral, J. M. Escola, D. P. Serrano, J. Přech, C. Ochoa-Hernández and J. Čejka, *Catal Sci Technol*, 2016, **6**, 2754–2765.

49 J. Socci, A. Osatiashtiani, G. Kyriakou and T. Bridgwater, *Appl Catal A Gen*, 2019, **570**, 218–227.

50 A. Marcilla, A. Gómez-Siurana and F. Valdés, *Polym Degrad Stab*, 2007, **92**, 197–204.

51 D. P. Serrano, J. Aguado and J. M. Escola, in *Catalysts: Volume 23*, Royal Society of Chemistry, 2011, pp. 253–283.

52 D. P. Serrano, J. M. Escola and P. Pizarro, *Chem Soc Rev*, 2013, **42**, 4004–4035.

53 D. Verboekend, J. C. Groen and J. Pérez-Ramírez, *Adv Funct Mater*, 2010, **20**, 1441–1450.

54 D. P. Serrano, J. Aguado, J. M. Escola, J. M. Rodríguez and A. Peral, *Chemistry of Materials*, 2006, **18**, 2462–2464.

55 Y. Zang, J. Wang, J. Gu, J. Qu, F. Gao and M. Li, *J Solid State Chem*, 2020, **291**, 121643.

56 M. Alonso-Doncel, A. Peral, M. Shamzhy, J. Čejka, R. Sanz and D. P. Serrano, *Microporous and Mesoporous Materials*, 2020, **303**, 110189.

57 Y. Zang, J. Wang, J. Gu, J. Qu and F. Gao, *CrystEngComm*, 2020, **22**, 3598–3607.

58 K. A. Tarach, K. Góra-Marek, J. Martinez-Triguero and I. Melián-Cabrera, *Catal Sci Technol*, 2017, **7**, 858–873.

59 D. P. Serrano, J. Aguado, J. M. Escola, J. M. Rodriguez and A. Peral, *J Catal*, 2010, **276**, 152–160.

60 S. Zhou, P. Li, H. Pan and Y. Zhang, *Ind Eng Chem Res*, 2022, **61**, 11407–11416.

61 G. Manos, I. Y. Yusof, N. Papayannakos and N. H. Gangas, *Ind Eng Chem Res*, 2001, **40**, 2220–2225.

62 G. Manos, I. Y. Yusof, N. H. Gangas and N. Papayannakos, *Energy and Fuels*, 2002, **16**, 485–489.

63 A. P. Pradeep and S. Gowthaman, *Fuel*, 2022, **323**, 124416.

64 A. Marcilla, A. Gómez-Siurana and D. Berenguer, *Appl Catal A Gen*, 2006, **301**, 222–231.

65 J. Aguado, J. L. Sotelo, D. P. Serrano, J. A. Calles and J. M. Escola, *Energy and Fuels*, 1997, **11**, 1225–1230.

66 J. Aguado, D. P. Serrano, G. S. Miguel, J. M. Escola and J. M. Rodríguez, *J Anal Appl Pyrolysis*, 2007, **78**, 153–161.

67 Y. Xue, P. Johnston and X. Bai, *Energy Convers Manag*, 2017, **142**, 441–451.

68 A. Eschenbacher, F. Goodarzi, R. J. Varghese, K. Enemark-Rasmussen, S. Kegnæs, M. S. Abbas-Abadi and K. M. Van Geem, *ACS Sustain Chem Eng*, 2021, **9**, 14618–14630.

69 A. Eschenbacher, R. J. Varghese, M. S. Abbas-Abadi and K. M. Van Geem, *Chemical Engineering Journal*, 2022, **428**, 132087.

70 A. Eschenbacher, R. J. Varghese, E. Delikonstantis, O. Mynko, F. Goodarzi, K. Enemark-Rasmussen, J. Oenema, M. S. Abbas-Abadi, G. D. Stefanidis and K. M. Van Geem, *Appl Catal B*, 2022, **309**, 121251.

71 J. Bozi and M. Blazsó, *J Anal Appl Pyrolysis*, 2012, **97**, 189–197.

72 G. Chen, T. Liu, P. Luan, N. Li, Y. Sun, J. Tao, B. Yan and Z. Cheng, *J Hazard Mater*, 2023, **453**, 131406.

73 D. P. Serrano, J. Aguado, J. M. Escola, J. M. Rodríguez, L. Morselli and R. Orsi, *J Anal Appl Pyrolysis*, 2003, **68–69**, 481–494.

74 J. Wang, J. Jiang, Y. Sun, X. Wang, M. Li, S. Pang, R. Ruan, A. J. Ragauskas, Y. S. Ok and D. C. W. Tsang, *J Clean Prod*, 2021, **309**, 127469.

75 M. Alonso-Doncel, A. Peral, M. Shamzhy, J. Čejka, R. Sanz and D. P. Serrano, *Microporous and Mesoporous Materials*, , DOI:10.1016/j.micromeso.2020.110189.

76 S. Du, J. A. Valla, R. S. Parnas and G. M. Bollas, *ACS Sustain Chem Eng*, 2016, **4**, 2852–2860.

77 A. Bohre, P. R. Jadhao, K. Tripathi, K. K. Pant, B. Likozar and B. Saha, *ChemSusChem*, 2023, **2023**, e202300142.

78 D. Yao, Y. Zhang, P. T. Williams, H. Yang and H. Chen, *Appl Catal B*, 2018, **221**, 584–597.

79 A. A. Aboul-Enein and A. E. Awadallah, *Chemical Engineering Journal*, 2018, **354**, 802–816.

80 M. Ibáñez, M. Artetxe, G. Lopez, G. Elordi, J. Bilbao, M. Olazar and P. Castaño, *Appl Catal B*, 2014, **148–149**, 436–445.

81 D. P. Serrano, J. Aguado, J. M. Rodríguez and A. Peral, *J Anal Appl Pyrolysis*, 2007, **79**, 456–464.

82 P. Castaño, G. Elordi, M. Ibañez, M. Olazar and J. Bilbao, *Catal Sci Technol*, 2012, **2**, 504–508.

83 G. Elordi, M. Olazar, P. Castaño, M. Artetxe and J. Bilbao, *Ind Eng Chem Res*, 2012, **51**, 14008–14017.

84 V. Daligaux, R. Richard and M.-H. Manero, *Catalysts*, 2021, **11**, 770.

85 D. P. Serrano, J. Aguado, J. M. Escola and E. Garagorri, *Appl Catal B*, 2003, **44**, 95–105.

86 *Stockholm Convention on Persistent Organic Pollutants. Item 5 (b)*, 2015.

87 Y. Shen, R. Zhao, J. Wang, X. Chen, X. Ge and M. Chen, *Waste Management*, 2016, **49**, 287–303.

88 C. Ma, J. Yu, B. Wang, Z. Song, J. Xiang, S. Hu, S. Su and L. Sun, *Renewable and Sustainable Energy Reviews*, 2016, **61**, 433–450.

89 M. R. Flid, L. M. Kartashov and Yu. A. Treger, *Catalysts*, 2020, **10**, 216.

90 H. Bockhorn, J. Hentschel, A. Hornung and U. Hornung, *Chem Eng Sci*, 1999, **54**, 3043–3051.

91 H. Bockhorn, A. Hornung, U. Hornung, P. Jakobströer and M. Kraus, *J Anal Appl Pyrolysis*, 1999, **49**, 97–106.

92 A. López, I. De Marco, B. M. Caballero, M. F. Laresgoiti and A. Adrados, *Fuel Processing Technology*, 2011, **92**, 253–260.

93 G. Yuan, D. Chen, L. Yin, Z. Wang, L. Zhao and J. Y. Wang, *Waste Management*, 2014, **34**, 1045–1050.

94 N. Dong, H. Hui, S. Li and L. Du, *J Anal Appl Pyrolysis*, 2023, **169**, 105817.

95 A. Marino, A. Aloise, H. Hernando, J. Fermoso, D. Cozza, E. Giglio, M. Migliori, P. Pizarro, G. Giordano and D. P. Serrano, *Catal Today*, 2022, **390–391**, 210–220.

96 J. Lei, G. Yuan, P. Weerachanchai, S. W. Lee, K. Li, J. Y. Wang and Y. Yang, *J Mater Cycles Waste Manag*, 2018, **20**, 137–146.

97 M. A. Keane, *Journal of Chemical Technology & Biotechnology*, 2007, **82**, 787–795.

98 D. Perondi, D. Restelatto, C. Manera, M. Godinho, A. J. Zattera and A. C. Faria Vilela, *Process Safety and Environmental Protection*, 2019, **122**, 58–67.

99 B. Fekhar, L. Gombor and N. Miskolczi, *Journal of the Energy Institute*, 2019, **92**, 1270–1283.

100 J. Yanik, M. A. Uddin, K. Ikeuchi and Y. Sakata, *Polym Degrad Stab*, 2001, **73**, 335–346.

101 C. Tang, Y. Z. Wang, Q. Zhou and L. Zheng, *Polym Degrad Stab*, 2003, **81**, 89–94.

102 D. Torres, Y. Jiang, D. A. Sanchez-Monsalve and G. A. Leeke, *J Anal Appl Pyrolysis*, 2020, **149**, 104831.

103 J. Hubáček, J. Lederer, P. Kuráň, P. Koutník, Z. Gholami, M. Zbuzek and M. Bačiak, *Fuel Processing Technology*, 2022, **231**, 107226.

104 M. Blazsó and Z. Czégény, *J Chromatogr A*, 2006, **1130**, 91–96.

105 T. Chen, J. Yu, C. Ma, K. Bikane and L. Sun, *Chemosphere*, 2020, **248**, 125964.

106 M. Brebu, T. Bhaskar, K. Murai, A. Muto, Y. Sakata and M. A. Uddin, *Polym Degrad Stab*, 2005, **87**, 225–230.

107 S. H. Jung, S. J. Kim and J. S. Kim, *Fuel*, 2012, **95**, 514–520.

108 R. Gao, B. Liu, L. Zhan, J. Guo, J. Zhang and Z. Xu, *J Hazard Mater*, 2020, **392**, 122447.

109 L. Ali, M. S. Kuttiyathil, O. H. Ahmed and M. Altarawneh, *Sep Purif Technol*, 2023, **307**, 122836.

110 N. Zhang, R. Li, G. Zhang, L. Dong, D. Zhang, G. Wang and T. Li, *ACS Omega*, 2020, **5**, 11987–11997.

111 A. Lopez-Urionabarrenechea, I. De Marco, B. M. Caballero, M. F. Laresgoiti and A. Adrados, *Fuel Processing Technology*, 2015, **137**, 229–239.

112 N. Lingaiah, M. A. Uddin, A. Muto, T. Imai and Y. Sakata, *Fuel*, 2001, **80**, 1901–1905.

113 N. Lingaiah, M. Azhar Uddin, A. Muto, Y. Sakata, T. Imai and K. Murata, *Appl Catal A Gen*, 2001, **207**, 79–84.

114 K.-R. Hwang, S.-A. Choi, I.-H. Choi and K.-H. Lee, *J Anal Appl Pyrolysis*, 2021, **155**, 105090.

115 G. Jiang, D. A. Sanchez Monsalve, P. Clough, Y. Jiang and G. A. Leeke, *ACS Sustain Chem Eng*, 2021, **9**, 1576–1589.

116 B. B. Uzoejinwa, X. He, S. Wang, A. El-Fatah Abomohra, Y. Hu and Q. Wang, *Energy Convers Manag*, 2018, **163**, 468–492.

117 B. Kunwar, H. N. Cheng, S. R. Chandrashekaran and B. K. Sharma, *Renewable and Sustainable Energy Reviews*, 2016, **54**, 421–428.

118 R. Palos, A. Gutiérrez, F. J. Vela, M. Olazar, J. M. Arandes and J. Bilbao, *Energy and Fuels*, 2021, **35**, 3529–3557.

119 V. I. Sharypov, N. Marin, N. G. Beregovtsova, S. V. Baryshnikov, B. N. Kuznetsov, V. L. Cebolla and J. V. Weber, *J Anal Appl Pyrolysis*, 2002, **64**, 15–28.

120 Y. Xue, S. Zhou, R. C. Brown, A. Kelkar and X. Bai, *Fuel*, 2015, **156**, 40–46.

121 H. Hassan, J. K. Lim and B. H. Hameed, *Bioresour Technol*, 2016, **221**, 645–655.

122 P. Lu, Q. Huang, A. C. (Thanos) Bourtsalas, Y. Chi and J. Yan, *Fuel*, 2018, **230**, 359–367.

123 E. M. Grieco and G. Baldi, *Waste Management*, 2012, **32**, 833–839.

124 J. Yu, L. Sun, C. Ma, Y. Qiao and H. Yao, *Waste Management*, 2016, **48**, 300–314.

125 Y. Matsuzawa, M. Ayabe and J. Nishino, *Polym Degrad Stab*, 2001, **71**, 435–444.

126 D. Czajczyńska, L. Anguilano, H. Ghazal, R. Krzyżyńska, A. J. Reynolds, N. Spencer and H. Jouhara, *Thermal Science and Engineering Progress*, 2017, **3**, 171–197.

127 F. Pinto, M. Miranda, I. Gulyurtlu and C. I, in *Recycling and Reuse of Used Tyres*, eds. R. Dhir, M. Limbachiya and K. Paine, Telford Ltd., 2001, pp. 27–38.

128 M. Miranda, P. Costa, F. Pinto, I. Gulyurtlu, A. Matos and I. Cabrita, in *Procedings of Energex*, 2004, pp. 125–129.

129 F. Paradela, F. Pinto, A. M. Ramos, I. Gulyurtlu and I. Cabrita, *J Anal Appl Pyrolysis*, 2009, **85**, 392–398.

130 Y. Wu, J. Zhu, Y. Wang, H. Yang, L. Jin and H. Hu, *Fuel*, 2021, **303**, 121199.

131 I. Kojić, A. Bechtel, N. Aleksić, D. Životić, S. Trifunović, G. Gajica and K. Stojanović, *Polymers (Basel)*, 2021, **13**, 1–25.

132 T. Zhang, W. Yuchi, Z. Bai, R. Hou, Z. Feng, Z. Guo, L. Kong, J. Bai, B. Meyer and W. Li, *J Clean Prod*, 2022, **333**, 130168.

133 T. Schubert, M. Lehner, T. Karner, W. Hofer and A. Lechleitner, *Fuel Processing Technology*, 2019, **193**, 204–211.

134 J. V. Milato, R. J. França, A. S. Rocha and M. R. C. M. Calderari, *J Anal Appl Pyrolysis*, 2020, **151**, 104928.

135 T. Schubert, A. Lechleitner, M. Lehner and W. Hofer, *Fuel*, 2020, **262**, 116597.

136 X. Zhang, H. Lei, S. Chen and J. Wu, *Green Chemistry*, 2016, **18**, 4145–4169.

137 L. Zhang, Z. Bao, S. Xia, Q. Lu and K. Walters, *Catalysts*, 2018, **8**, 659.

138 X. Chen, Q. Che, S. Li, Z. Liu, H. Yang, Y. Chen, X. Wang, J. Shao and H. Chen, *Fuel Processing Technology*, 2019, **196**, 106180.

139 X. Zhang, H. Lei, L. Zhu, X. Zhu, M. Qian, G. Yadavalli, D. Yan, J. Wu and S. Chen, *Bioresour Technol*, 2016, **214**, 45–54.

140 Y. Xue, A. Kelkar and X. Bai, *Fuel*, 2015, **166**, 227–236.

141 B. Fekhar, V. Zsinka and N. Miskolczi, *J Environ Manage*, 2020, **269**, 110741.

142 X. Zhang, H. Lei, L. Zhu, M. Qian, X. Zhu, J. Wu and S. Chen, *Appl Energy*, 2016, **173**, 418–430.

143 M. H. M. Ahmed, N. Batalha, H. M. D. Mahmudul, G. Perkins and M. Konarova, *Bioresour Technol*, 2020, **310**, 123457.

144 X. Lin, H. Lei, E. Huo, M. Qian, W. Mateo, Q. Zhang, Y. Zhao, C. Wang and E. Villota, *Energy Convers Manag*, 2020, **211**, 112757.

145 M. H. M. Ahmed, N. Batalha, T. Qiu, M. M. Hasan, L. Atanda, N. Amiralian, L. Wang, H. Peng and M. Konarova, *J Hazard Mater*, 2020, **396**, 122711.

146 M. Qian, H. Lei, E. Villota, Y. Zhao, E. Huo, C. Wang, W. Mateo and R. Zou, *Energy Convers Manag*, 2021, **236**, 114020.

147 Y. Bin, Z. Yu, M. Li, Z. Huang, J. Zhan, Y. Liao, A. Zheng and X. Ma, *J Anal Appl Pyrolysis*, 2022, **167**, 105673.

148 T. Nandakumar, U. Dwivedi, K. K. Pant, S. Kumar and E. Balaraman, *Catal Today*, 2023, **408**, 111–126.

149 P. Das and P. Tiwari, *Thermochim Acta*, 2017, **654**, 191–202.

150 F. Xu, B. Wang, D. Yang, J. Hao, Y. Qiao and Y. Tian, *Energy Convers Manag*, 2018, **171**, 1106–1115.

151 A. Aboulkas, K. El harfi, A. El bouadili, M. Nadifiyine, M. Benchanaa and A. Mokhlisse, *Fuel Processing Technology*, 2009, **90**, 722–728.

152 A. Aboulkas, K. El harfi and A. El Bouadili, *Energy Convers Manag*, 2010, **51**, 1363–1369.

153 L. S. Diaz Silvarrey and A. N. Phan, *Int J Hydrogen Energy*, 2016, **41**, 16352–16364.

154 P. Kannan, J. J. Biernacki, D. P. Visco and W. Lambert, *J Anal Appl Pyrolysis*, 2009, **84**, 139–144.

155 Y. Mo, L. Zhao, C. L. Chen, G. Y. A. Tan and J. Y. Wang, *J Therm Anal Calorim*, 2013, **111**, 781–788.

156 R. Tuffi, S. D'Abramo, L. M. Cafiero, E. Trinca and S. Vecchio Ciprioti, *Express Polym Lett*, 2018, **12**, 82–99.

157 Z. Wang, T. Xie, X. Ning, Y. Liu and J. Wang, *Waste Management*, 2019, **99**, 146–153.

158 H. Liu, C. Wang, J. Zhang, W. Zhao and M. Fan, *Energy and Fuels*, 2020, **34**, 2385–2390.

159 J. M. Criado, *Thermochim Acta*, 1978, **24**, 186–189.

160 S. M. Al-Salem and P. Lettieri, *Chemical Engineering Research and Design*, 2010, **88**, 1599–1606.

161 S. M. Al-Salem, *Process Safety and Environmental Protection*, 2019, **127**, 171–179.

162 G. Elordi, G. Lopez, M. Olazar, R. Aguado and J. Bilbao, *J Hazard Mater*, 2007, **144**, 708–714.

163 S. Pyo, Y. M. Kim, Y. Park, S. B. Lee, K. S. Yoo, M. Ali Khan, B. H. Jeon, Y. Jun Choi, G. Hoon Rhee and Y. K. Park, *Journal of Industrial and Engineering Chemistry*, 2021, **103**, 136–141.

164 A. Coelho, I. M. Fonseca, I. Matos, M. M. Marques, A. M. Botelho do Rego, M. A. N. D. A. Lemos and F. Lemos, *Appl Catal A Gen*, 2010, **374**, 170–179.

165 A. Coelho, L. Costa, M. M. Marques, I. M. Fonseca, M. A. N. D. A. Lemos and F. Lemos, *Appl Catal A Gen*, 2012, **413–414**, 183–191.

166 R. Singhal, C. Singhal and S. Upadhyayula, *J Anal Appl Pyrolysis*, 2010, **89**, 313–317.

167 B. Saha, P. Chowdhury and A. K. Ghoshal, *Appl Catal B*, 2008, **83**, 265–276.

168 Y. H. Lin and M. H. Yang, *Thermochim Acta*, 2008, **470**, 52–59.

169 A. Durmuş, S. N. Koç, G. S. Pozan and A. Kaşgöz, *Appl Catal B*, 2005, **61**, 316–322.

170 J. S. Kim, W. Y. Lee, S. B. Lee, S. B. Kim and M. J. Choi, *Catal Today*, 2003, **87**, 59–68.

171 Y. M. Kim, S. Pyo, H. Hakimian, K. S. Yoo, G. H. Rhee and Y. K. Park, *Sustainability (Switzerland)*, 2021, **13**, 13386.

172 I. Kremer, T. Tomić, Z. Katančić, M. Erceg, S. Papuga, J. P. Vuković and D. R. Schneider, *J Environ Manage*, 2021, **296**, 113145.

173 W. C. Huang, M. S. Huang, C. F. Huang, C. C. Chen and K. L. Ou, *Fuel*, 2010, **89**, 2305–2316.

174 Z. Till, T. Varga, J. Sója, N. Miskolczi and T. Chován, *Energy Convers Manag*, 2018, **173**, 320–330.

175 F. Campuzano, R. C. Brown and J. D. Martínez, *Renewable and Sustainable Energy Reviews*, 2019, **102**, 372–409.

176 M. L. Mastellone and U. Arena, *AIChE Journal*, 2002, **48**, 1439–1447.

177 D. Macrì, K. Cassano, A. Pierro, A. Le Pera, E. Giglio, E. Muraca, P. Farinelli, C. Freda, E. Catizzone, G. Giordano and M. Migliori, *Fuel Processing Technology*, 2022, **233**, 107297.

178 Q. Xiong, Y. Yang, F. Xu, Y. Pan, J. Zhang, K. Hong, G. Lorenzini and S. Wang, *ACS Sustain Chem Eng*, 2017, **5**, 2783–2798.

179 J. Zavala-Gutiérrez, O. Pérez-Camacho, L. Villarreal-Cárdenas and E. Saldívar-Guerra, *Ind Eng Chem Res*, 2019, **58**, 19050–19060.

180 A. Niksiar and M. Sohrabi, *J Anal Appl Pyrolysis*, 2014, **110**, 66–78.

181 L. A. De la Flor-Barriga and U. F. Rodríguez-Zúñiga, *RSC Adv*, 2022, **12**, 12436–12445.

182 A. Gala, D. Catalán-Martínez, M. Guerrero and J. M. Serra, *Fuel*, 2021, **287**, 119400.

183 M. M. Wright, D. E. Daugaard, J. A. Satrio and R. C. Brown, *Fuel*, 2010, **89**, S2–S10.

184 S. L. Wong, N. Ngadi, T. A. T. Abdullah and I. M. Inuwa, *Renewable and Sustainable Energy Reviews*, 2015, **50**, 1167–1180.

185 G. C. Faussone, *Waste Management*, 2018, **73**, 416–423.

186 S. Belbessai, A. Azara and N. Abatzoglou, *Processes*, 2022, **10**, 733.

187 E. Rodríguez, A. Gutiérrez, R. Palos, F. J. Vela, J. M. Arandes and J. Bilbao, *Waste Management*, 2019, **93**, 162–172.

188 K. H. Lee, *J Anal Appl Pyrolysis*, 2012, **94**, 209–214.

189 J. R. Banu, V. G. Sharmila, U. Ushani, V. Amudha and G. Kumar, *Science of the Total Environment*, 2020, **718**, 137287.

190 I. Hita, A. T. Aguayo, M. Olazar, M. J. Azkoiti, J. Bilbao, J. M. Arandes and P. Castaño, *Energy and Fuels*, 2015, **29**, 7542–7553.

191 K. Ragaert, L. Delva and K. Van Geem, *Waste Management*, 2017, **69**, 24–58.

192 F. Ding, C. Luo, H. Zhang, L. Xiong and X. D. Chen, *Pet Sci Technol*, 2015, **33**, 1846–1852.

193 M. Solis and S. Silveira, *Waste Management*, 2020, **105**, 128–138.

194 L. Santamaria, G. Lopez, E. Fernandez, M. Cortazar, A. Arregi, M. Olazar and J. Bilbao, *Energy and Fuels*, 2021, **35**, 17051–17084.

195 R. Krzywda and B. Wrzesińska, *Waste Biomass Valorization*, 2021, **12**, 91–104.

196 M. J. McIntosh, G. G. Arzoumanidis and F. E. Brockmeier, *Environmental Progress*, 1998, **17**, 19–23.

197 J. N. Sahu, K. K. Mahalik, H. K. Nam, T. Y. Ling, T. S. Woon, M. S. bin Abdul Rahman, Y. K. Mohanty, N. S. Jayakumar and S. S. Jamuar, *Environ Prog Sustain Energy*, 2014, **33**, 298–307.

198 H. Y. Ismail, A. Abbas, F. Azizi and J. Zeaiter, *Waste Management*, 2017, **60**, 482–493.

199 A. Fivga and I. Dimitriou, *Energy*, 2018, **149**, 865–874.

200 A. Somoza-Tornos, A. Gonzalez-Garay, C. Pozo, M. Graells, A. Espuña and G. Guillén-Gosálbez, *ACS Sustain Chem Eng*, 2020, **8**, 3561–3572.

201 R. W. J. Westerhout, M. P. Van Koningsbruggen, A. G. J. Van Der Ham, J. A. M. Kuipers and W. P. M. Van Swaaij, *Chemical Engineering Research and Design*, 1998, **76**, 427–439.

202 G. Jiang, J. Wang, S. M. Al-Salem and G. A. Leeke, *Energy and Fuels*, 2020, **34**, 7397–7409.

203 D. G. Kulas, A. Zolghadr, U. S. Chaudhari and D. R. Shonnard, *J Clean Prod*, 2023, **384**, 135542.

204 A. Serras-Malillos, E. Acha, A. Lopez-Urionabarrenechea, B. B. Perez-Martinez and B. M. Caballero, *Chemosphere*, 2022, **300**, 134499.

205 H. Almohamadi, M. Alamoudi, U. Ahmed, R. Shamsuddin and K. Smith, *Korean Journal of Chemical Engineering*, 2021, **38**, 2208–2216.